



NARSIS

New Approach to Reactor Safety Improvements

WP2: Fragility assessment of main NPPs critical elements

Del. 2.7: Derivation of hazard-harmonized fragility models



This project has received funding from the Euratom research and training programme 2014-2018 under Grant Agreement No. 755439.



Project Acronym: NARSIS
Project Title: New Approach to Reactor Safety Improvements
Deliverable: Del. 2.7: Derivation of hazard-harmonized fragility models
Month due: 45 **Month delivered:** 54
Leading Partner: BRGM
Version: V1

Primary Authors: Florent DE MARTIN, Pierre GEHL (BRGM)

Other contributors:

-

Deliverable Review:

- **Reviewer #1:** E. Foerster (CEA) **Date:**
- **Reviewer #2:** P. Vardon (TU Delft) **Date:**

Dissemination Level		
PU	Public	X
PP	Restricted to other programme participants (including the Commission Services)	
RE	Restricted to a group specified by the consortium (including the Commission Services)	
CO	Confidential, only for members of the consortium (including the Commission Services)	

Table of contents

1	Executive Summary	6
2	Introduction	7
3	Dyke’s geometrical and mechanical properties	8
4	Dyke’s factor of safety	9
5	Input ground motions	9
6	Numerical modelling of the dyke	12
7	Earthquake-flooding scenario.....	13
8	Volcanic eruption-mainshock-aftershock scenario	17
9	Design of multi-hazard fragility models	20
9.1	Definition of damage states and fragility modelling assumptions	20
9.2	Earthquake-flooding fragility model	20
9.3	Volcanic eruption-mainshock-aftershock fragility model.....	22
10	Conclusions	26
11	References.....	27
	Appendix: FLAC/FISH configuration file of the “earthquake-flooding” scenario.....	28

List of Figures

Figure 1: Geometry and material of the dyke composed by a clay core (light blue), gravelly sand shells (green and red) overlaying an elastic bedrock (purple).....	8
Figure 2: Factor of safety of the dyke computed with the “strength reduction method”.....	9
Figure 3: Example of drift correction. Time series without drift correction (black), time series with drift correction (red).....	10
Figure 4: Frequency content of the set of accelerograms used in this study.....	11
Figure 5: Response spectra of the accelerograms database of this study.....	11
Figure 6: PGA (left y-axis) and PGV (right y-axis) of the dataset of ground motions.....	11
Figure 7: Spectral ratio between the base and the top of the dyke: fundamental frequency visible around 20 Hz and 1 st higher mode around 35 Hz (FD grid set up to be valid up to 40 Hz for this computation only).....	12
Figure 8: Comparison of the velocities simulated inside the core of the dyke, 2.5 m below the top, with a grid of 1m (solid black line) and a grid of 2 m (solid red line) for EQ16x2.....	12
Figure 9: Sequence of computations steps in the earthquake-flooding scenario.....	13
Figure 10: Stress field (S_{yy} in Pa) after dyke construction stage.....	14
Figure 11: Pore-pressure (in Pa) field at steady state flow for reservoir raised to mid dyke elevation.....	14
Figure 12: X-displacement field (in m) at the static-equilibrium reached after the water weight loading.....	15
Figure 13: Y-displacement field (in m) at the static-equilibrium after the water weight loading (end of step S1-1).....	15
Figure 14: X-displacement (in meter) after earthquake n°91 (end of step S1-2).....	15
Figure 15: Y-displacement (in meter) after earthquake n°91 (end of step S1-2).....	16
Figure 16: Maximum residual X-displacement vs. PGA, within the dyke at the end of the seismic loading (step S1-2). Filled circle: set n°1 of accelerograms. Empty square: set n°2 of accelerograms.....	16
Figure 17: Maximum residual Y-displacement vs. PGA, within the dyke at the end of the seismic loading (step S1-2). Filled circle: set n°1 of accelerograms. Empty square: set n°2 of accelerograms.....	16
Figure 18: Sequence of computations steps in the volcanic eruption-mainshock-aftershock scenario.....	17
Figure 19: Maximum residual X-displacement within the dyke after the mainshock (S2-3) and after the sequence mainshock-aftershock (S2-4).....	18
Figure 20: Maximum residual Y-displacement within the dyke after the mainshock (S2-3, empty circles) and after the sequence mainshock-aftershock (S2-4, filled circle).....	18
Figure 21: Maximum residual X-displacement within the dyke after the sequence mainshock-aftershock without tephra loading (filled circles) and with various tephra loadings (filled triangles, empty squares and crosses).....	18
Figure 22: Effective shear stresses σ'_{xx} (top left panel) and σ'_{yy} : top panels are after step S2-1 and bottom panels, after step S2-2.....	19
Figure 23: Maximum residual Y-displacement within the dyke after the sequence mainshock-aftershock without tephra loading (filled circles) and with various tephra loadings (filled triangles, empty squares and crosses).....	19
Figure 24: Relative difference between d_{xy} at step S1-2 (EQ alone) and at step S1-3 (EQ + flooding), with respect to the seismic intensity measure PGA.....	21
Figure 25: Fragility functions for the earthquake-flooding scenario, without the flooding (Left) and with the flooding (Right).....	21
Figure 26: Bayesian Network for the construction of multi-hazard fragility models.....	23

Figure 27: Probability of being in states DS ₁ (Left) and DS ₂ (Right) with respect to mainshock PGA (PGA MS) and tephra load (TL), with no aftershock.	24
Figure 28: Probability of being in states DS ₁ (Left) and DS ₂ (Right) with respect to mainshock PGA (PGA MS) and tephra load (TL), with aftershock PGA = 3.64 m/s ²	24
Figure 29: Probability of being in states DS ₁ (Left) and DS ₂ (Right) with respect to mainshock PGA (PGA MS) and tephra load (TL), with aftershock PGA = 7.42 m/s ²	25
Figure 30: Probability of being in states DS ₁ (Left) and DS ₂ (Right) with respect to mainshock PGA (PGA MS) and tephra load (TL), with aftershock PGA = 11.21 m/s ²	25
Figure 31: Probability of being in states DS ₁ (Left) and DS ₂ (Right) with respect to mainshock PGA (PGA MS) and aftershock PGA (PGA AS), with no tephra load.....	25
Figure 32: Probability of being in states DS ₁ (Left) and DS ₂ (Right) with respect to mainshock PGA (PGA MS) and aftershock PGA (PGA AS), with tephra load TL = 40 kPa.	25

List of Tables

Table 1: Fragility parameters estimated for the earthquake-flooding scenario.	21
Table 2: Fragility parameters estimated for the tephra loading.	22
Table 3: Fragility parameters estimated for the mainshock, given various levels of tephra loading.	22
Table 4: Conditional fragility parameters estimated for the aftershock, given DS ₁ during the mainshock, and given various levels of tephra loading. Larger tephra loads are not considered here because they do not result in the occurrence of DS ₂	23

1 Executive Summary

This deliverable report presents the results of task 2.3 regarding the fragility analyses performed on one of the main critical elements of Nuclear Power Plants (NPP) as identified by task 2.1. The critical element under study is a dyke protecting the plant site from flooding. It is composed of a clay core surrounded by upstream and downstream compacted sand. Investigated external hazard events are sequences of earthquake/flooding and volcanic eruption/earthquake mainshock/aftershock.

2 Introduction

While the generation of multi-hazard events has been addressed in WP1 of the NARSIS project, multi-risk interactions have also to be considered at the fragility level, in order to account for the damages that are potentially accumulated from joint or subsequent hazard loadings. Such effects cannot be taken into account by the combination of single-hazard fragility curves, since some hazard loadings will have the effect of altering the state of the structural system and its structural response to subsequent loading.

One of the first of these models is the one developed by Lee & Rosowsky (2006), who consider the combined effect of snow and earthquake loadings on wood frame buildings. Parametric seismic fragility curves are derived for different values of snow load on the rooftop, thus resulting in a fragility surface expressing the probability of failure with respect to seismic intensity and snow load. Similar considerations are investigated by Zuccaro et al. (2008), who propose vulnerability models that account for cumulated damages during volcanic eruptions. More specifically, the effect of volcanic ash load on the rooftop is quantified with respect to earthquakes and pyroclastic flows: no fragility curves are developed, but load multiplier coefficients or updated vulnerability classes are proposed as inputs to damage probability matrices. In the case of bridges, the combined effects of scour and earthquakes have become a popular subject in the last few years. For instance, through vibration monitoring on an Italian roadway bridge, Foti & Sabia (2011) have demonstrated the impact of scour on the dynamic response of the structure. It is shown that modal identification may be used as a powerful tool to locate and monitor the evolution of scour at bridge piers. On the other hand, Prasad and Banerjee (2013) have used non-linear time-history analyses to compute fragility curves for RC bridge piers subjected to various levels of scour: the results are presented as a response surface, which shows the evolution of the fragility median with respect to the scour depth and the diameter of the equivalent foundation pile. Alipour et al. (2012) have also used non-linear bridge models to derive parametric fragility curves for various scour depths. The probability of failure due to the combined effects of scour and earthquakes during the design lifetime of the bridge can then be quantified: it is represented as a joint probability density function of scour depth and PGA, which can be compared with the maximum acceptable probability of failure given by design codes in order to obtain scour load-modification factors.

More recently, a study by Gehl & D'Ayala (2016) has developed a Bayesian Network (BN) framework in order to build multi-hazard fragility model, applied to a RC bridge. This approach is applied here to the fragility analysis of a dyke protecting the plant site from flooding. It is composed of a clay core surrounded by upstream and downstream compacted sand. Investigated external hazard events are sequences of earthquake/flooding and volcanic eruption/earthquake mainshock/aftershock.

3 Dyke's geometrical and mechanical properties

The shape of the canonical dyke used in this study is inspired from those damaged during the Niigata earthquake, 1964, Japan (Kawakami, 1966). The dyke is supposed to be made of a low-permeability homogeneous clay core zone with upstream and downstream homogeneous gravelly sand shells. The basement of the dyke is at elevation $y = 0$ m and its crest at elevation $y = 5$ m (Figure 1). The crest is 10 m wide and the base 40 m wide. The slope of the shells is 1:3 and the one of the core 1:1. It is constructed above a homogeneous bedrock, such as sandstone, which shear modulus is 8.5 GPa, bulk modulus is 17.7 GPa and density is 2500 kg/m³. The corresponding P and S-wave velocities for the bedrock are $V_s = 1844$ m/s and $V_p = 3408$ m/s. The bedrock is supposed linear elastic while the clay and gravelly sand's rheology are elastic perfectly plastic with a Mohr-Coulomb (MC) yielding criterion. The shear modulus of the dyke's core is 1.731 GPa, the bulk modulus 3.75 GPa and density is 1800 kg/m³. The corresponding P and S-wave velocities are $V_s = 981$ m/s and $V_p = 1834$ m/s. The MC properties are the cohesion = 4 kPa, the friction angle = 35°, the dilation angle = 0° and the tension = 0 Pa. The shear modulus of the dyke's shells is 0.288 GPa, the bulk modulus 0.768 GPa and density is 1800 kg/m³. The corresponding P and S-wave velocities are $V_s = 300$ m/s and $V_p = 800$ m/s. The MC properties are identical to those of the core. The permeability of the core and shells follows the FLAC convention and is defined as the conventional hydraulic conductivity divided by the unit weight of water. The FLAC permeability of the clay core is then 1.0E-11 m²/Pa.s, and the one of the shells and bedrock 1.0E-9 m²/Pa.s.

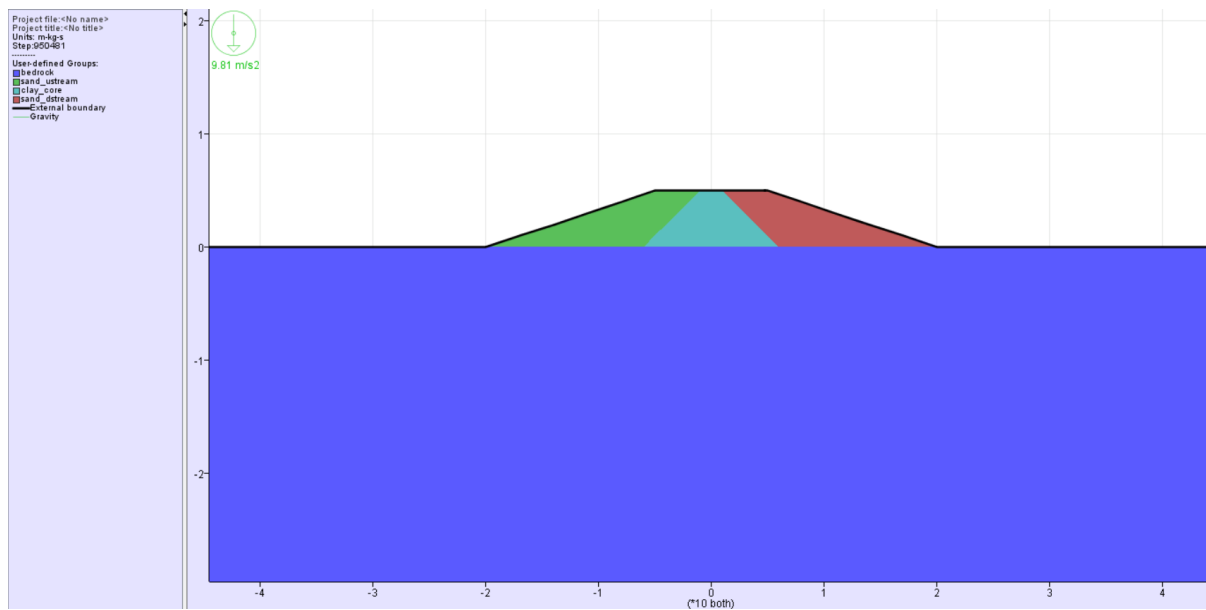


Figure 1: Geometry and material of the dyke composed by a clay core (light blue), gravelly sand shells (green and red) overlaying an elastic bedrock (purple).

4 Dyke's factor of safety

The computation of the factor of safety (FoS) of the dyke is based on the so-called “strength reduction method” (e.g., Dawson and Roth, 1999) by reducing the cohesion and the friction angle of the MC materials until failure occurs. The computation of the FoS takes place after the step n°1 described in Section 0, i.e., after the initialisation of new static-equilibrium conditions due to the water weight. The computation leads to a FoS value of 2.79 (Figure 2). This value is high but consistent with the conservative design of the dyke. As seen on Figure 2, the potential failure occurs within the downstream gravelly sand shell.

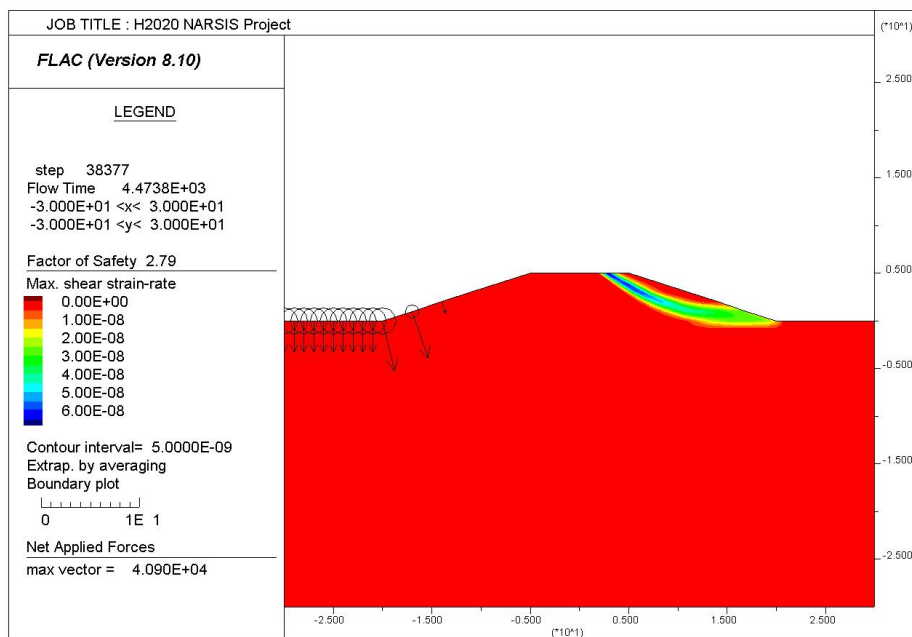


Figure 2: Factor of safety of the dyke computed with the “strength reduction method”.

5 Input ground motions

Accelerograms used in this study come from the NGA2West database, such as the 1994 Northridge earthquake, the 2004 Niigata earthquake, the 2009 L'Aquila earthquake, etc. They are ordered in 5 sets of 10 accelerograms (i.e., 50 in total), each set with an increasing response spectrum intensity at the period $T_1 = 0.33$ s (fundamental period of the main NPP reactor) based on the conditional mean spectrum method (Lin et al., 2013). They have been processed prior to the dynamic analysis to remove very-low (< 0.1 Hz) and very-high (> 30 Hz) frequencies, as well as displacement drift, if any (Figure 3). The displacement drift pre-processing has been done by the Seismic Analysis Code (SAC, Goldstein et al., 2003). The accelerograms from the database have been tapered, integrated to velocity, tapered integrated to displacement, high-passed by a 0.1 Hz corner frequency double-pass 4-poles Butterworth filter to remove displacement drift, tapered and differentiated to velocity and acceleration. The resulting velocity after differentiation has been de-convoluted of the free surface effect (i.e., division by a factor of two in case of homogeneous bedrock) before being injected at the bottom of the domain of simulation by using the standard zero-order stress boundary approximation (Clayton and Engquist, 1977).

An inspection of the Fourier spectrum of the set of accelerograms (Figure 4) shows that the main energy is located between 0.1 and 10 Hz. The energy after 15 Hz has been neglected for design of the numerical grid of the simulations in order to gain computational time. Figure 5 shows their acceleration response spectra. The peak ground acceleration (PGA) and peak ground velocity (PGV) of the dataset are depicted in Figure 6.

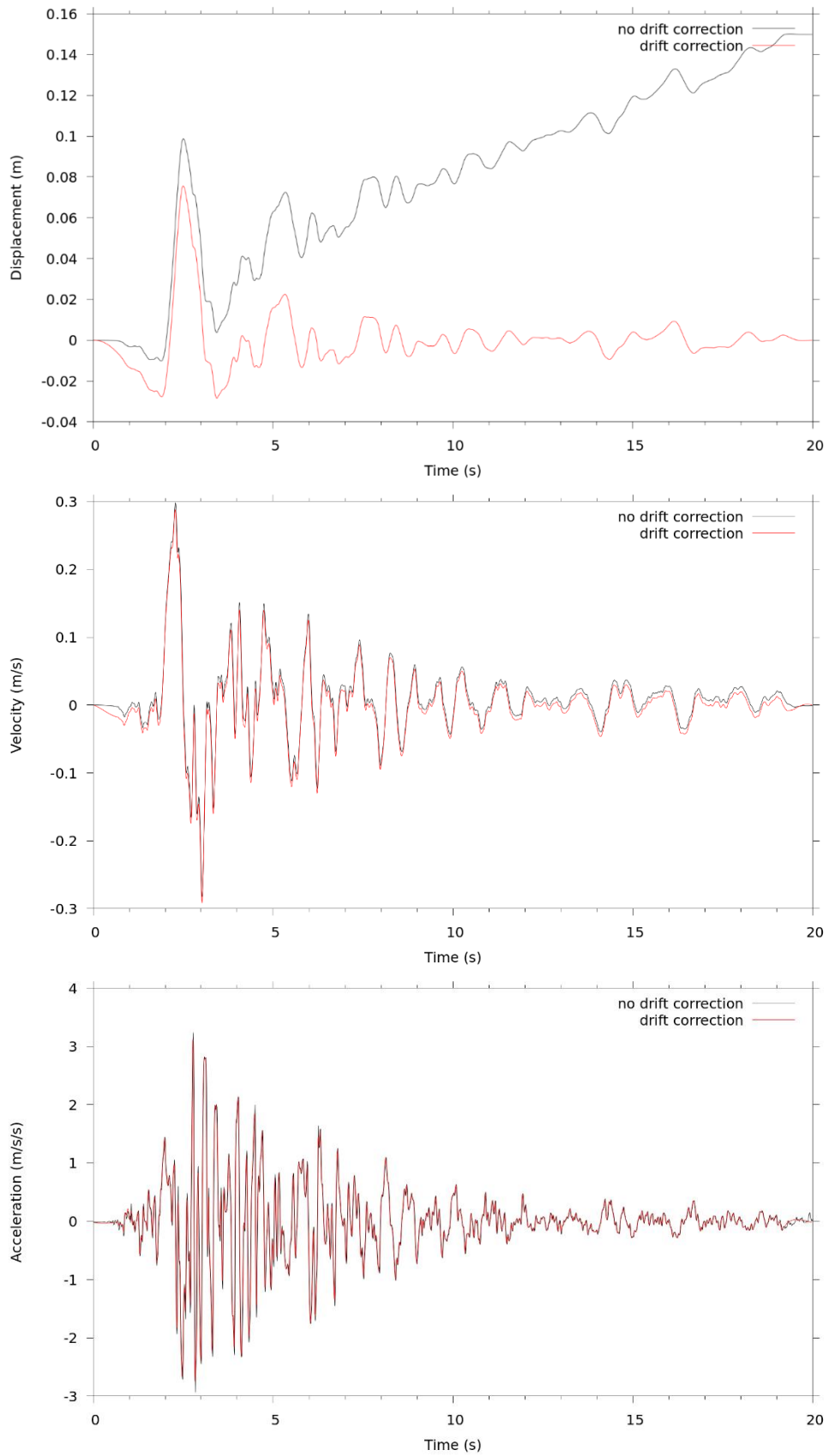


Figure 3: Example of drift correction. Time series without drift correction (black), time series with drift correction (red).

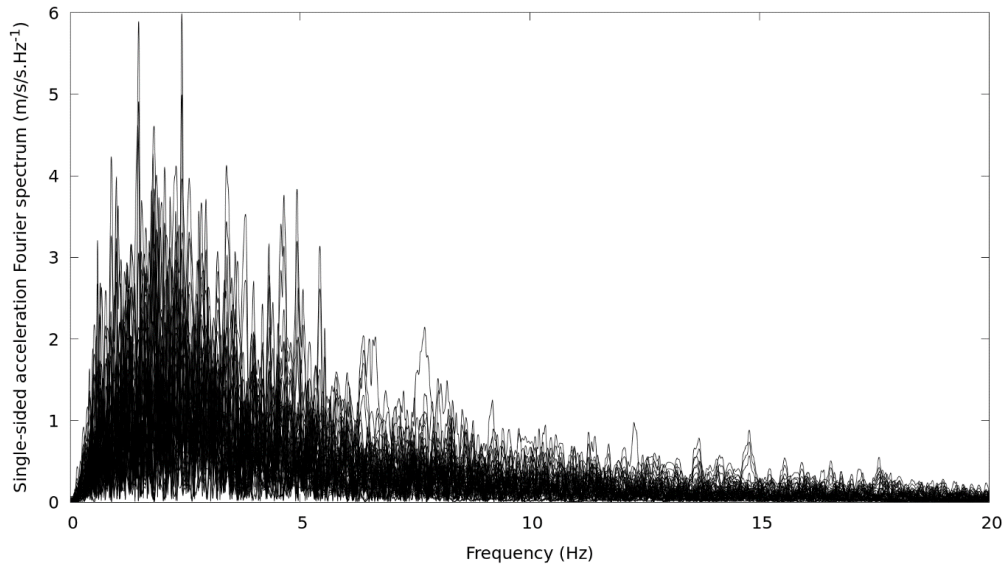


Figure 4: Frequency content of the set of accelerograms used in this study.

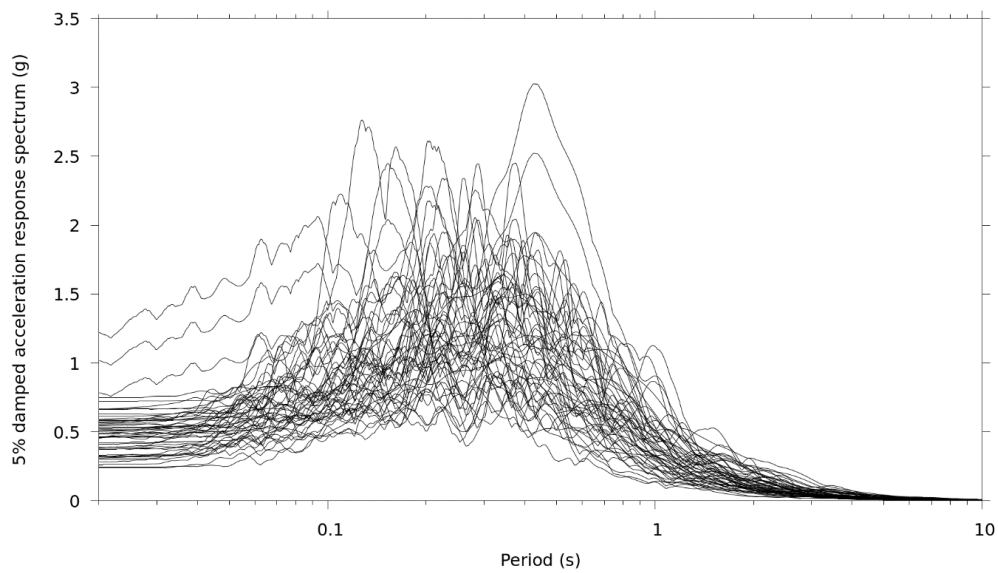


Figure 5: Response spectra of the accelerograms database of this study.

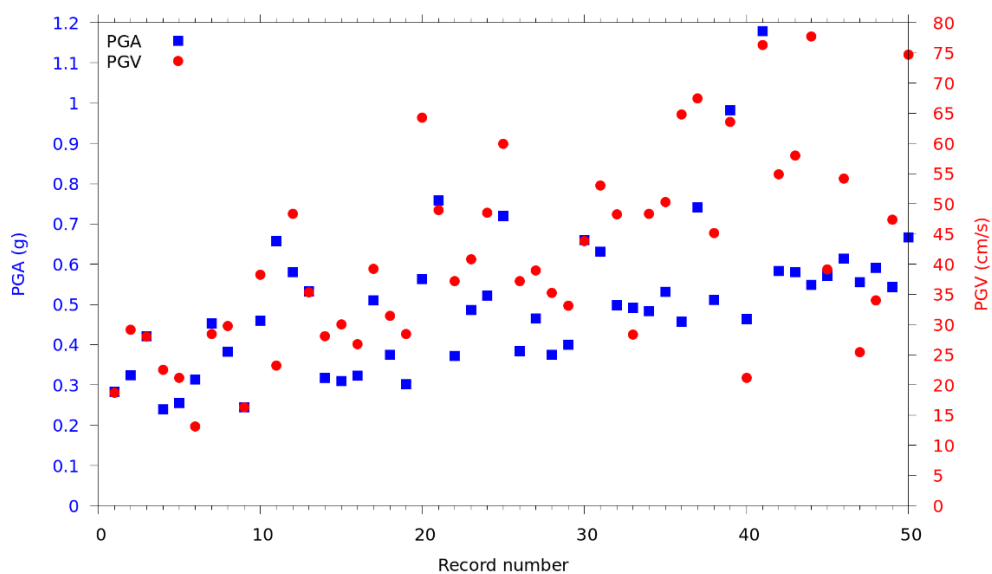


Figure 6: PGA (left y-axis) and PGV (right y-axis) of the dataset of ground motions.

6 Numerical modelling of the dyke

The dyke is modelled by a finite difference method (FDM) with the FLAC software (Itasca Consulting Group, 2019). The definition of its geometry and the associated discrete FD grid has been coded in FLAC/FISH language (see Appendix). The geometry, the size of the FD grid, the receivers location, the water level rise elevation or the earthquake input ground motion are configurable in FLAC/FISH configuration file. The computations performed for this study are valid up to 15 Hz using at least 8 grid points per minimal wavelength (the minimal wavelength is present in the shells with a value equal to $300/15 = 20$ m).

We note that the fundamental frequency of the dyke, located around 20 Hz (Figure 7), is not included in the valid frequency range of the FD grid, but its inclusion or not has no effect on the predicted ground motion (Figure 8). However, reducing the valid frequency down to 15 Hz allows for a substantial gain in computational time: a rough refinement over the entire domain of simulation from a grid step of 2 m to 1 m allows for a gain of 10 in computational time. A refinement of the dyke only has not been investigated.

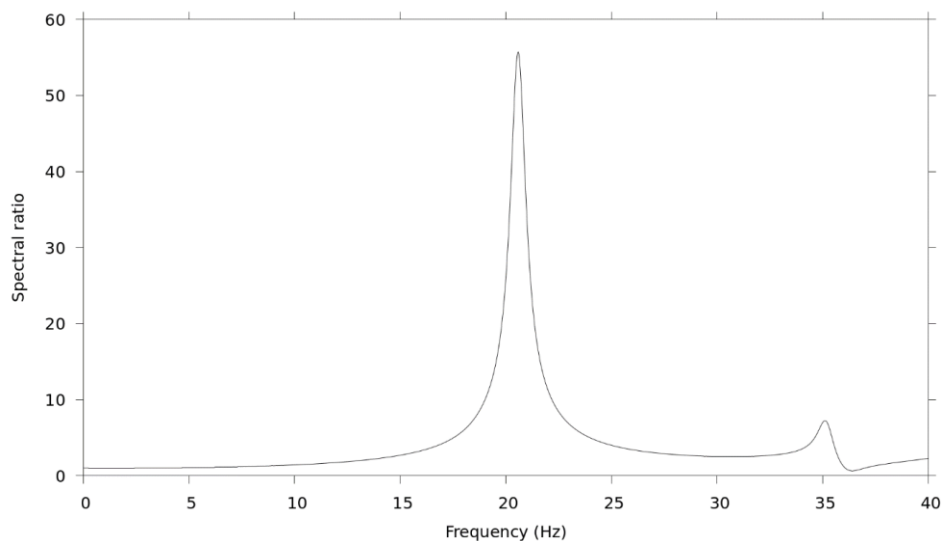


Figure 7: Spectral ratio between the base and the top of the dyke: fundamental frequency visible around 20 Hz and 1st higher mode around 35 Hz (FD grid set up to be valid up to 40 Hz for this computation only).

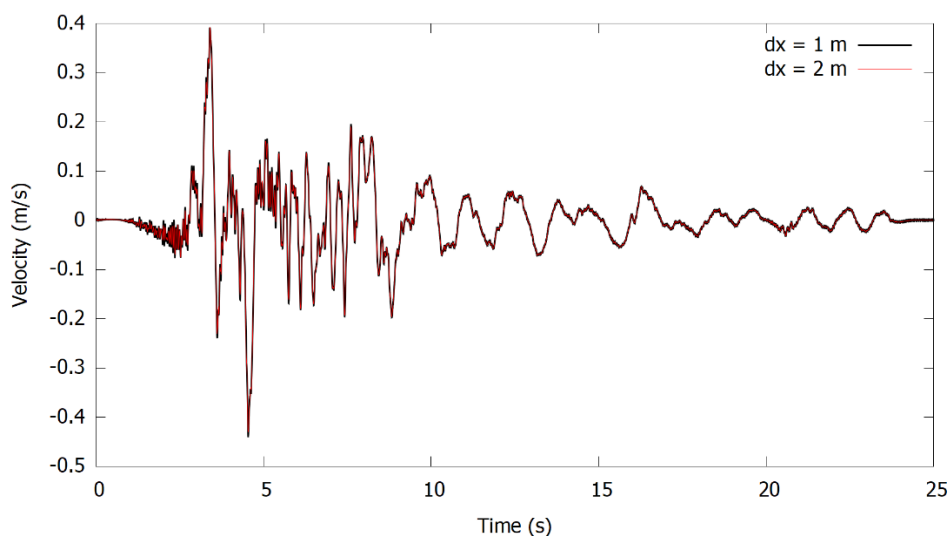


Figure 8: Comparison of the velocities simulated inside the core of the dyke, 2.5 m below the top, with a grid of 1m (solid black line) and a grid of 2 m (solid red line) for EQ16x2.

7 Earthquake-flooding scenario

As shown in Figure 9, this multi-hazard “earthquake-flooding” scenario considers three steps of loading involving the site-specific coupled groundwater static-equilibrium conditions before earthquake, the earthquake computed as a fully dynamic process, and finally a water level rise on the dyke’s upstream reservoir potentially due to a failure of an upstream construction (e.g., dam, dyke, etc.). In this scenario, the excess pore pressures is assumed to dissipate before the earthquake loading because of the long return period considered (i.e., 200 000 yr, see below).

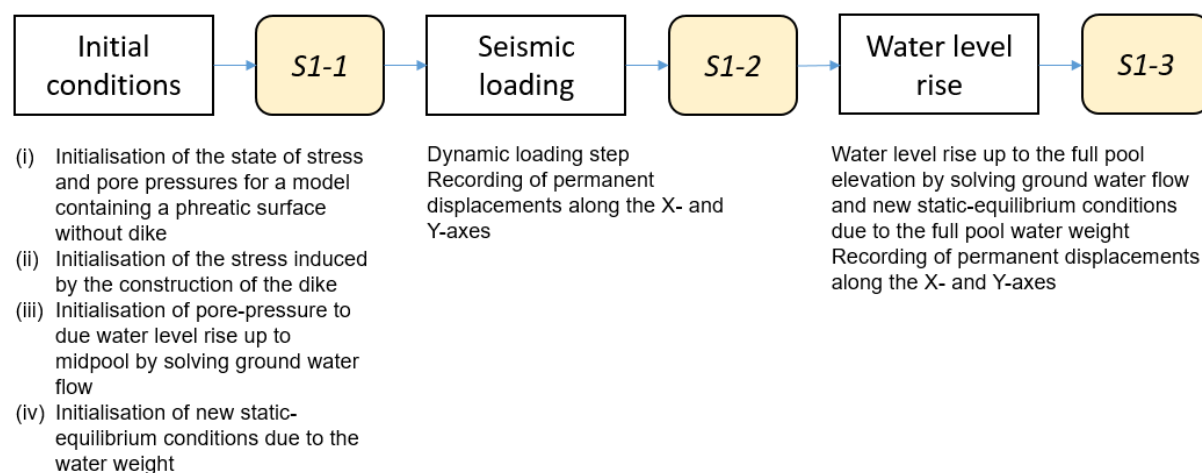


Figure 9: Sequence of computations steps in the earthquake-flooding scenario.

The first step (called S1-1 for “scenario 1-step 1”) consists in computing the state of stress under static conditions prior to the dynamic seismic loading. It includes (i) the initialisation of the state of stress and pore pressures for a model containing a phreatic surface without the dyke, (ii) the initialisation of the stress induced by the construction of the dyke (Figure 10), (iii) the initialisation of the pore-pressure to due water level rise up to mid-pool by solving ground water flow (Figure 11), and (iv) the initialisation of new static-equilibrium conditions due to the water weight (Figure 12 and Figure 13).

The second step (S1-2) consists in the seismic loading of the dyke by considering an increasing level of earthquake intensity using the above-mentioned conditional mean spectrum method. To this end, 100 accelerograms extracted from the NGA2West database have been employed to load the dyke. The first 50 accelerograms (also called set n°1) are those presented in Section 5 and correspond to a return period up to 200 000 years. The last 50 ones (also called set n°2) are the first 50 accelerograms scaled by a factor of two. We note that for sake of simplicity, we have neglected the source-spectrum versus magnitude dependency because the fundamental frequency of the dyke (see Figure 7) is much higher than the peak energy frequencies of our accelerograms dataset (see Figure 4) and consequently, the frequency content of the dataset should not influence the dynamic response of the dyke. For this dynamic loading step, the groundwater flow is not solved because it is assumed that the dynamic excitation occurs over a much smaller timeframe than required for pore pressures to dissipate. Figure 12 and Figure 13 show an example of permanent displacements along the X and Y-axis, respectively, after the dyke has been subjected to the earthquake n°91 (i.e., earthquake n°41 scaled by a factor of 2).

The third step (S1-3) consists in a water level rise up to the full pool elevation (5 m high) that would correspond to a 5000 years flooding return period. This step is performed by solving ground water flow and new static-equilibrium conditions due to the full pool water weight. Similar permanent displacement than those observed after the earthquake loading are

generally observed at the end this step, meaning that the static water level rise considered in this study could be neglected.

The maximum residual X and Y-displacements after the step S1-3 for both sets of accelerograms are depicted in Figure 16 and Figure 17, respectively.

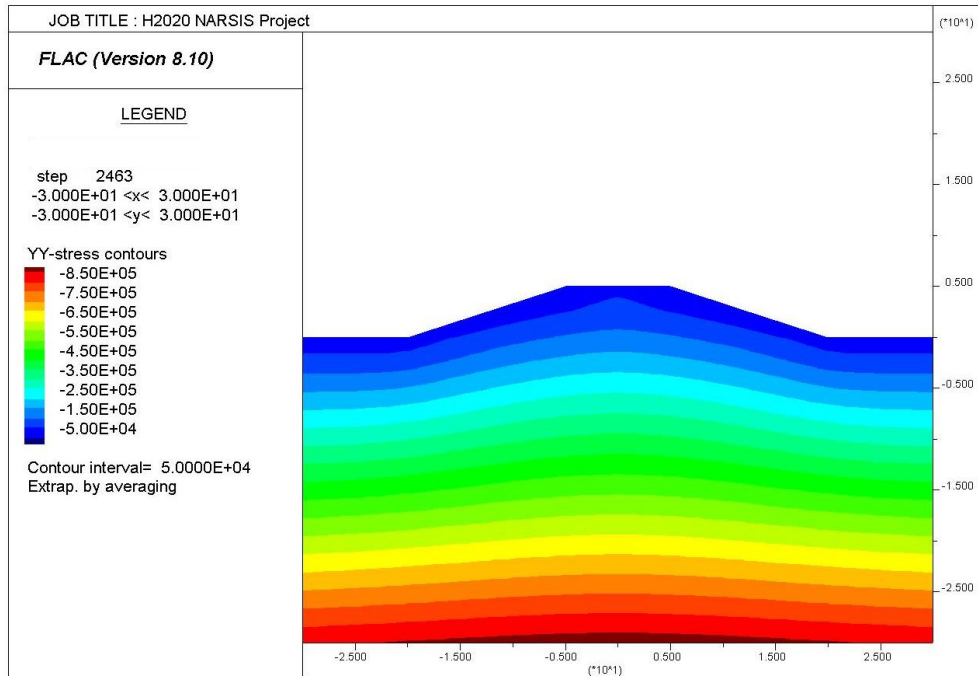


Figure 10: Stress field (S_{yy} in Pa) after dyke construction stage.

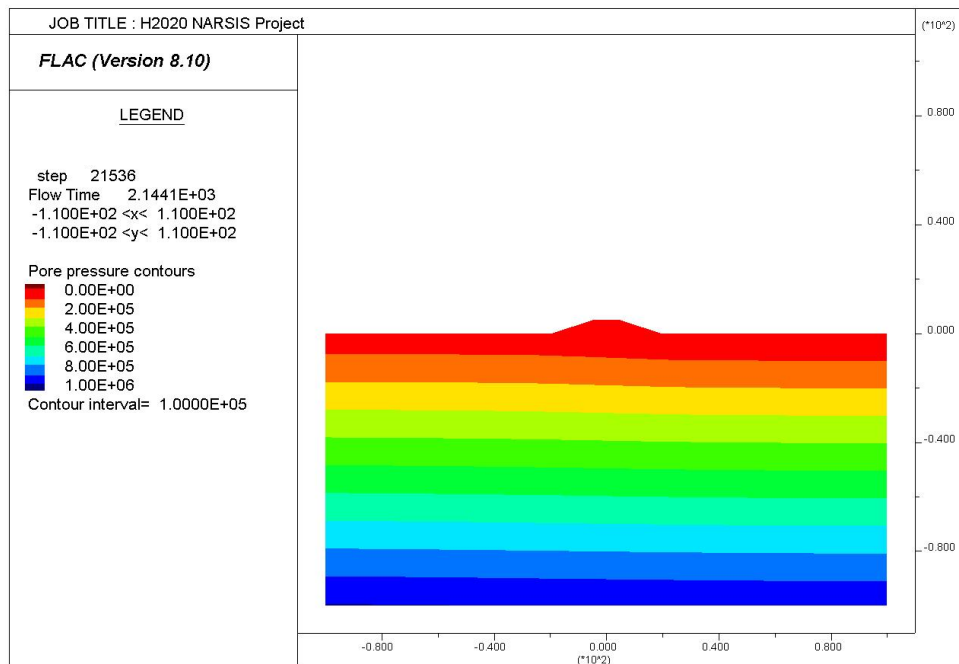


Figure 11: Pore-pressure (in Pa) field at steady state flow for reservoir raised to mid dyke elevation.

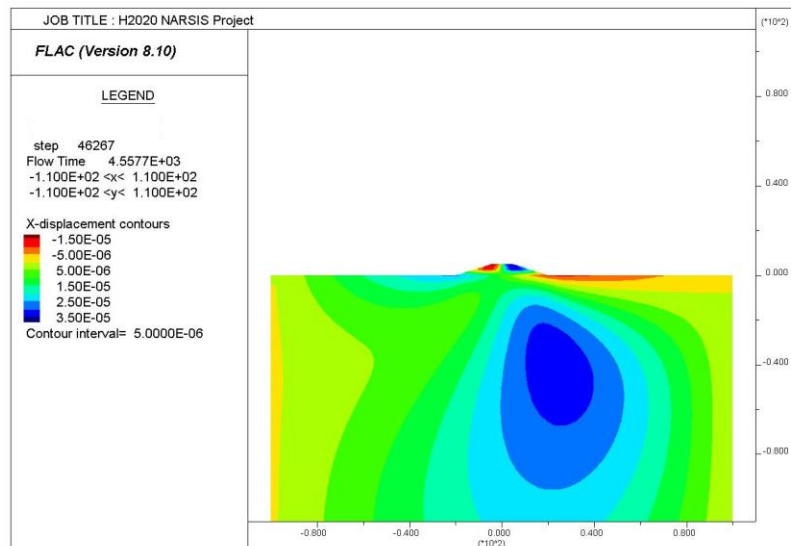


Figure 12: X-displacement field (in m) at the static-equilibrium reached after the water weight loading.

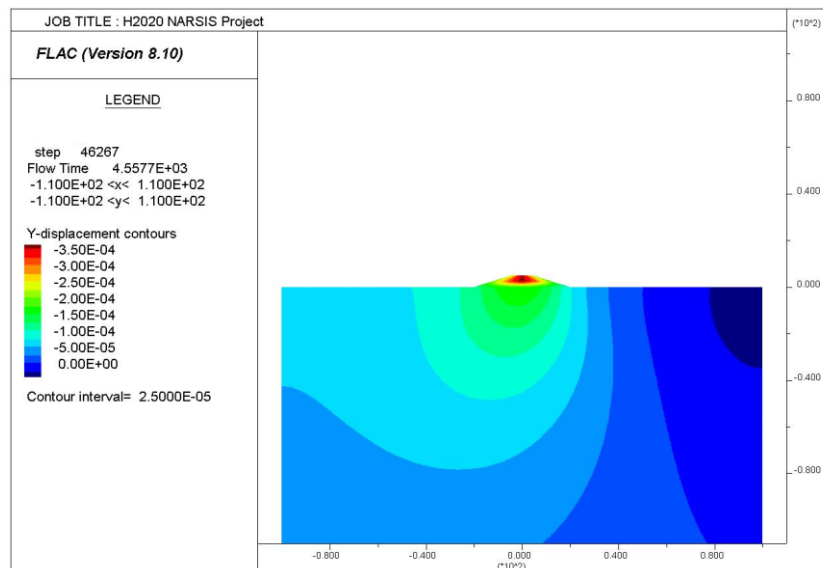


Figure 13: Y-displacement field (in m) at the static-equilibrium after the water weight loading (end of step S1-1).

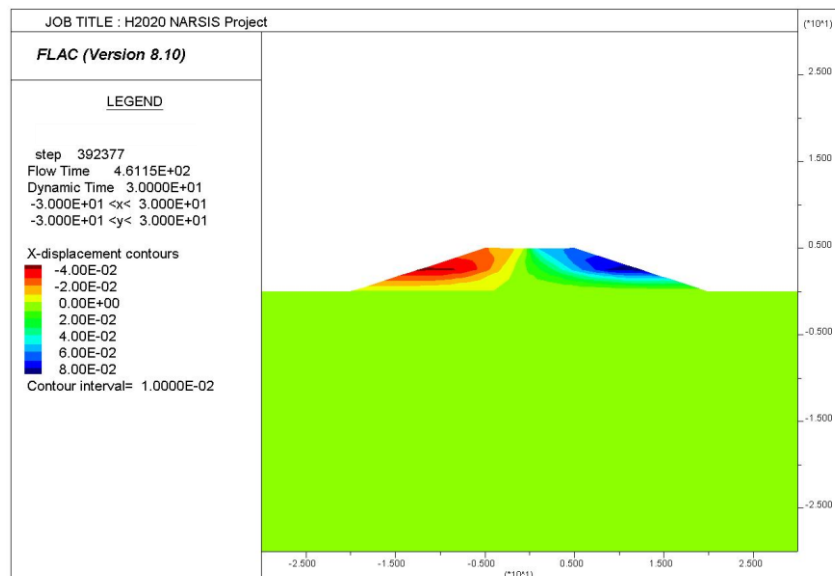


Figure 14: X-displacement (in meter) after earthquake n°91 (end of step S1-2).

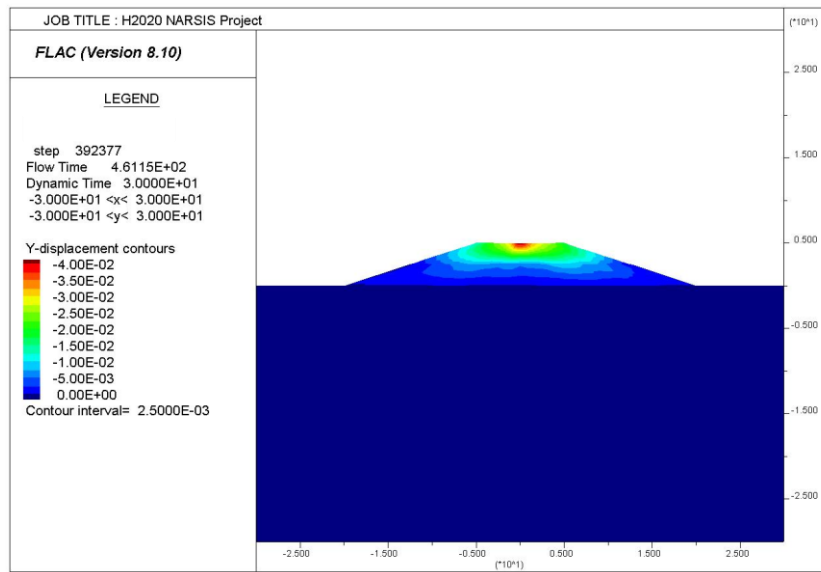


Figure 15: Y-displacement (in meter) after earthquake n°91 (end of step S1-2).

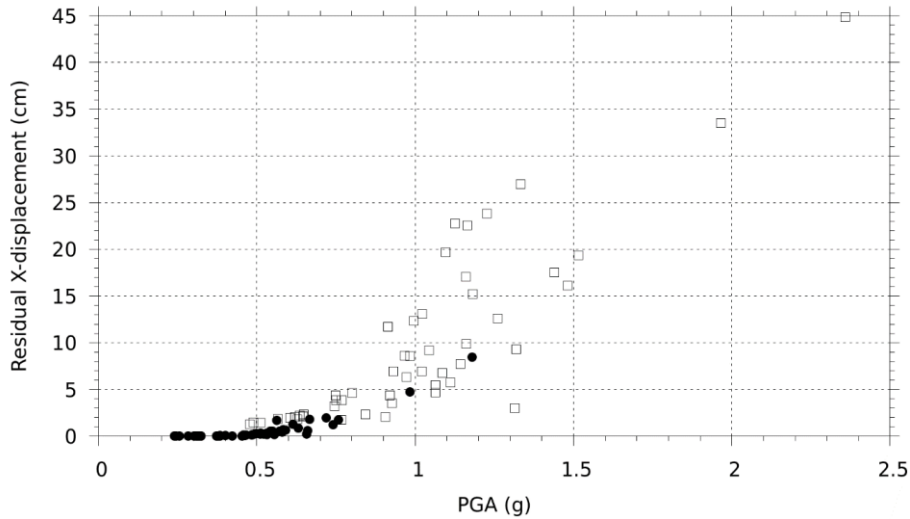


Figure 16: Maximum residual X-displacement vs. PGA, within the dyke at the end of the seismic loading (step S1-2). Filled circle: set n°1 of accelerograms. Empty square: set n°2 of accelerograms.

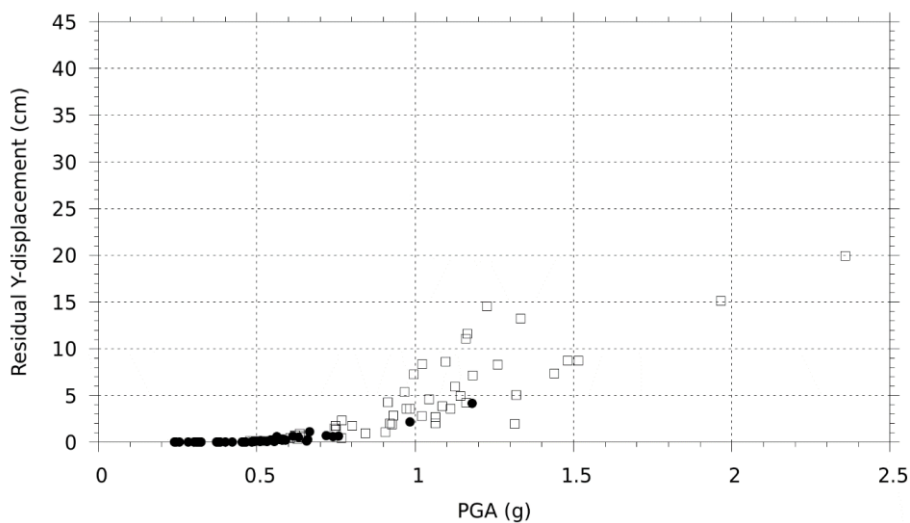


Figure 17: Maximum residual Y-displacement vs. PGA, within the dyke at the end of the seismic loading (step S1-2). Filled circle: set n°1 of accelerograms. Empty square: set n°2 of accelerograms.

8 Volcanic eruption-mainshock-aftershock scenario

This multi-hazard “volcanic eruption-mainshock-aftershock” scenario considers the following sequence of events (see Figure 18): the dyke’s site, supposed at its coupled groundwater static-equilibrium, is first subjected to a 100,000 years return period volcano eruption releasing a massive quantity of pyroclastic airfall deposits (tephra) falling on the dyke. Then, an active seismic fault produces two severe ground shakings near the dyke. The first ground shaking, considered as the mainshock, is related to the main strain energy release corresponding up to a 200 000 years return period and is followed up by a major aftershock (all other aftershocks are considered much smaller and are neglected for this case). In this scenario, the excess pore pressures is assumed to dissipate before mainshock because of the long return period considered, but is present when the major aftershock occurs.

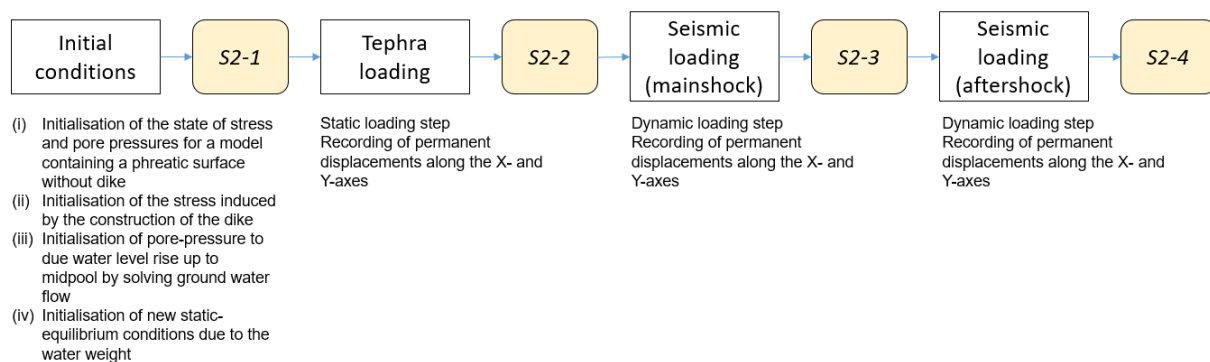


Figure 18: Sequence of computations steps in the volcanic eruption-mainshock-aftershock scenario.

In the same way as the “earthquake-flooding” scenario, the first step (called step S2-1 for “scenario 2 – step 1”, which is identical to step S1-1 presented in Section 0) consists in computing the site-specific coupled groundwater static-equilibrium conditions before the volcanic eruption. This step is followed by tephra loading (step S2-2) varying from 40 kPa to 140 kPa depending on the quantity of tephra falling on the site. A static mechanical pressure models the tephra deposit on the site. We note that this step can be omitted if the tephra loading is not considered. The mainshock (step S2-3) and aftershock (step S2-4) correspond to the sets of accelerograms n°2 and n°1, respectively. As for the step S1-2 presented in Section 0, the earthquake sequence is computed as a fully dynamic process.

By omitting the step S2-2 (i.e., no tephra loading), the maximum residual displacement within the dyke at the end of the steps S2-3 (mainshock only) and S2-4 (mainshock+aftershock) is depicted in Figure 19 for the X-component and in Figure 20 for the Y-component. For the X-component, we see that most of the aftershocks increase the maximum residual displacement. For the Y-component, the settlements after the sequence mainshock-aftershock are larger or equal to the settlements obtained after the mainshock.

By including the step S2-2, the maximum residual displacements within the dyke are always reduced compared to the case without tephra loading (see Figure 21 and Figure 23). This is due to the fact that the pressure exerted by the tephra deposits increases the effective stresses σ'_{xx} and σ'_{yy} within the clay and gravelly sand’s shells (see Figure 22) and consequently allows for larger effective shear stress before reaching the Mohr-Coulomb failure envelope. Under our current modelling hypotheses, the tephra deposits thus prevent the failure of the shells and large residual displacement within the dyke.

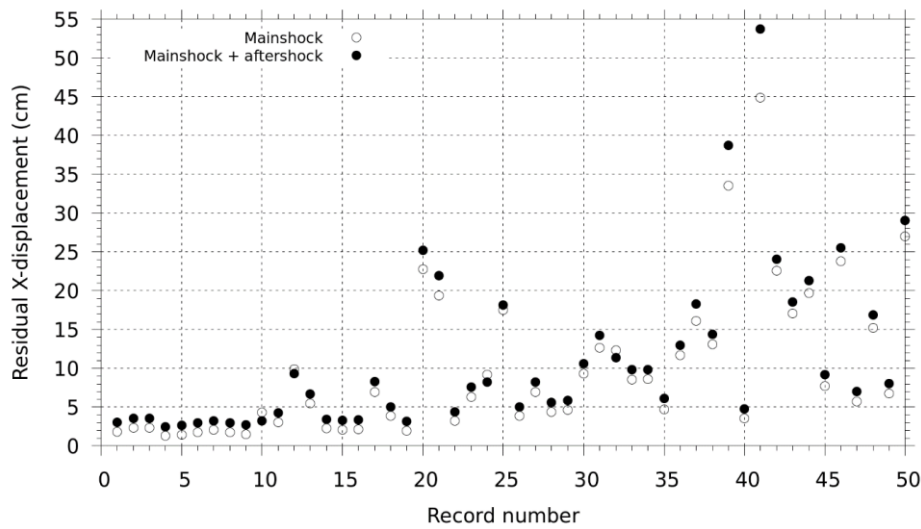


Figure 19: Maximum residual X-displacement within the dyke after the mainshock (S2-3) and after the sequence mainshock-aftershock (S2-4).

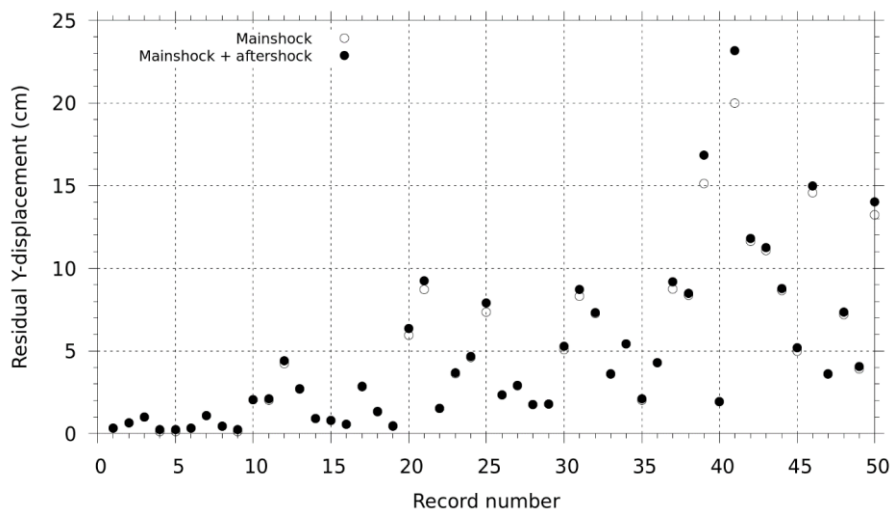


Figure 20: Maximum residual Y-displacement within the dyke after the mainshock (S2-3, empty circles) and after the sequence mainshock-aftershock (S2-4, filled circle).

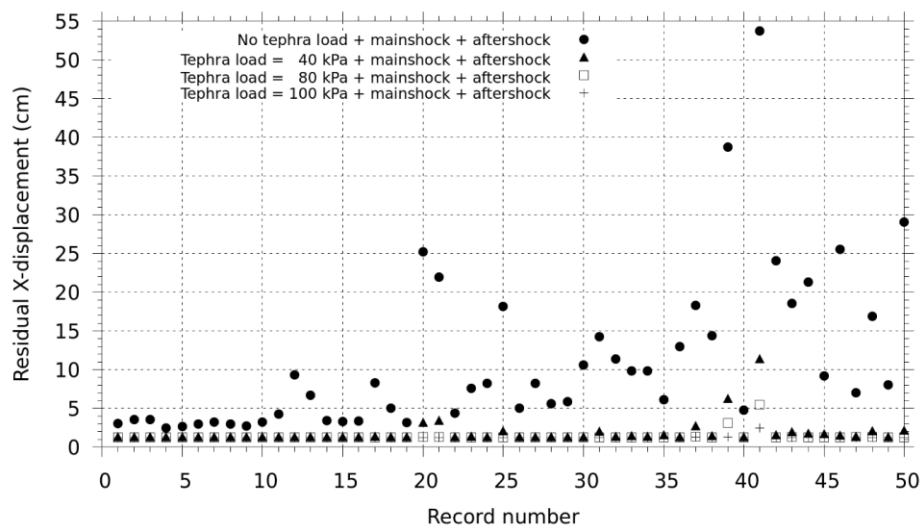


Figure 21: Maximum residual X-displacement within the dyke after the sequence mainshock-aftershock without tephra loading (filled circles) and with various tephra loadings (filled triangles, empty squares and crosses).

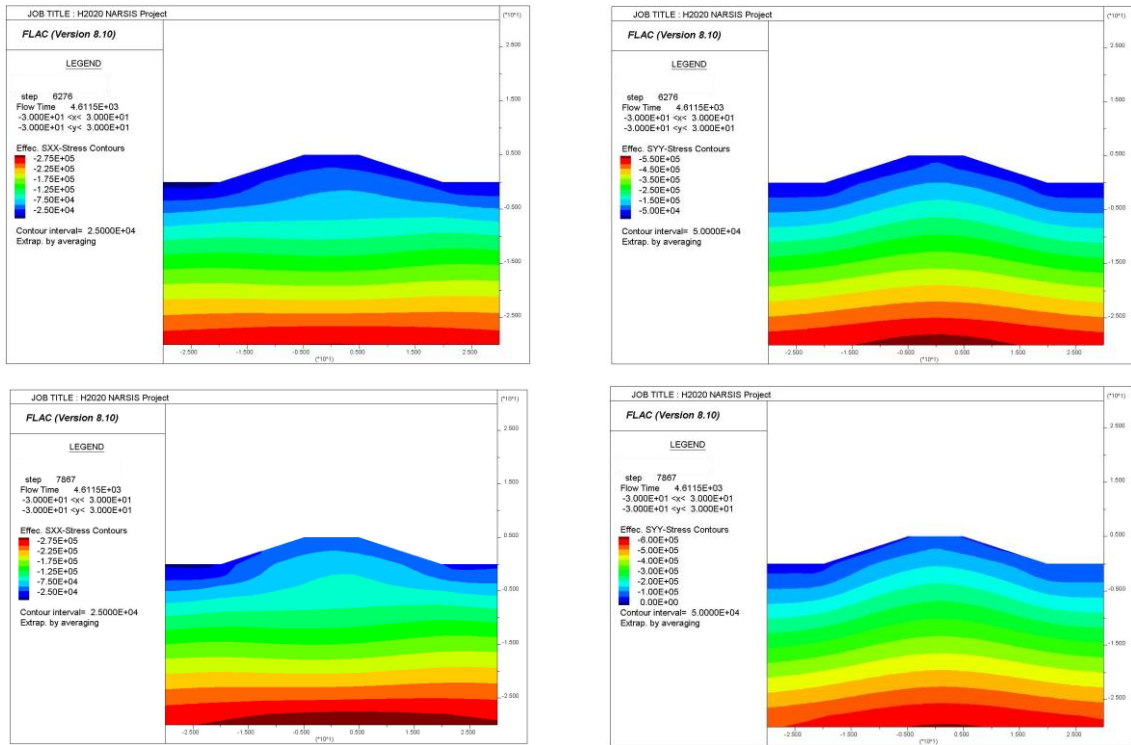


Figure 22: Effective shear stresses σ'_{xx} (top left panel) and σ'_{yy} : top panels are after step S2-1 and bottom panels, after step S2-2.

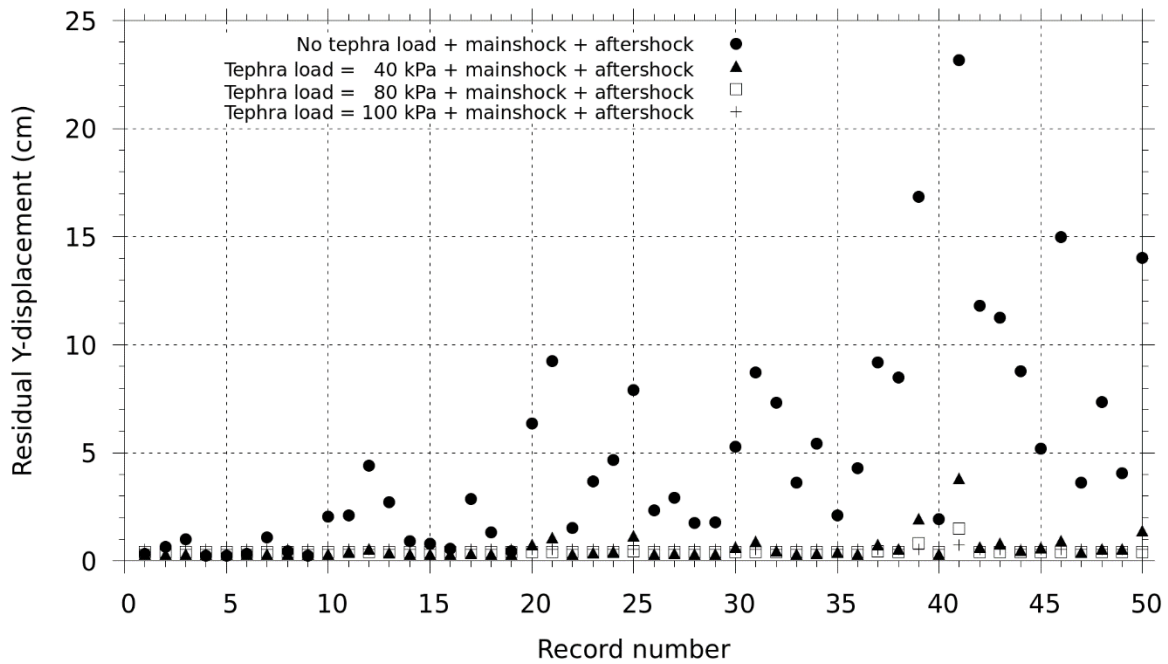


Figure 23: Maximum residual Y-displacement within the dyke after the sequence mainshock-aftershock without tephra loading (filled circles) and with various tephra loadings (filled triangles, empty squares and crosses).

9 Design of multi-hazard fragility models

This section demonstrates the derivation of multi-hazard fragility functions, applied to the two scenarios described above.

9.1 Definition of damage states and fragility modelling assumptions

The objective of the fragility analysis is to assess the capacity of the dyke to ensure its protective function with respect to the NPP site. Therefore, the failure, or extensive damage, to the dyke may be identified by the occurrence of large permanent displacements. Besides, the occurrence of very small permanent displacements, while not immediately threatening for the integrity of the dyke, should be identified in order to trigger inspections or minor repair actions. Therefore, two damage states are proposed here, corresponding to the following limit states expressed as d_{XY} , the maximum residual displacement over both directions:

- DS₁, minor damage: $d_{XY} = 0.001$ m;
- DS₂, extensive damage: $d_{XY} = 0.1$ m.

In the following sub-sections, the fragility functions are derived by following the framework developed in Task 2.3 and detailed in Deliverable Report D2.6. Fragility functions are assumed to follow a lognormal functional form:

$$P_f(im) = P(ds \geq DS | IM = im) = \Phi\left(\frac{\ln im - \ln \alpha}{\beta}\right) \quad (1)$$

where im is the intensity measure (IM) used in the fragility model, Φ is the standard normal cumulative distribution function, α is the median fragility parameter, and β the standard deviation parameter. The statistical method based on the least-squares regression ('regression on a cloud'), as described in NARSIS deliverable D2.6, is adopted here due to the relatively limited number of data points provided by the FLAC analyses.

9.2 Earthquake-flooding fragility model

In the first multi-hazard scenario (see Figure 9), it is possible to investigate the influence of hydraulic loading (i.e., flooding up to the crest of the dyke) after an earthquake loading. The results from the FLAC analyses reveal a very limited contribution of static hydraulic loading to the final residual displacements, which are mostly dominated by the earthquake loading. The relative impact of hydraulic loading is illustrated in Figure 24: the relative contribution is negligible for moderate to high levels of seismic intensity measure, while it remains noticeable at low levels (i.e., around 5%-10% of difference at $PGA < 5$ m/s²).

As a result, the fragility parameters are summarized in Table 1 and the corresponding fragility functions are plotted in Figure 26.

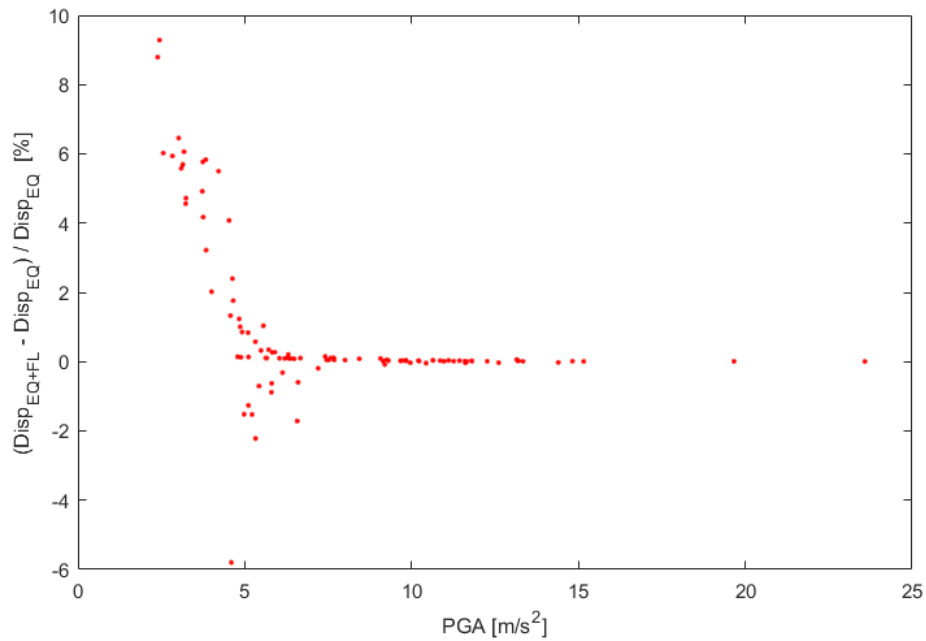


Figure 24: Relative difference between d_{xy} at step S1-2 (EQ alone) and at step S1-3 (EQ + flooding), with respect to the seismic intensity measure PGA.

Table 1: Fragility parameters estimated for the earthquake-flooding scenario.

	Earthquake (S1-2)		Earthquake + Flooding (S1-3)	
	α [m/s ²]	β	α [m/s ²]	β
DS₁	4.1813	0.2297	4.1503	0.2362
DS₂	11.4189	0.1748	11.4005	0.1742

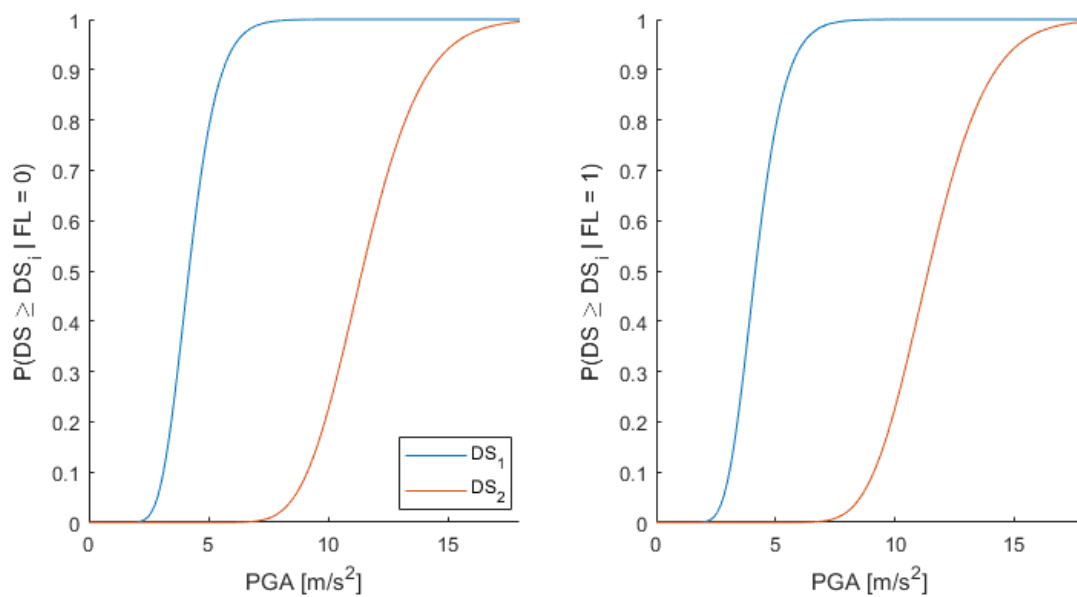


Figure 25: Fragility functions for the earthquake-flooding scenario, without the flooding (Left) and with the flooding (Right).

As expected, the differences are very slight between the flooding/no-flooding cases, although they are more visible for the DS₁ limit state. This scenario constitutes an example of the derivation of parametric fragility functions, where single-IM fragility curves (here, seismic fragility curves) are adjusted depending on the occurrence of a given event (here, the subsequent flooding).

9.3 Volcanic eruption-mainshock-aftershock fragility model

In the second multi-hazard scenario (see Figure 18), the contribution of multiple loadings needs to be considered:

- Tephra static loading (TL);
- Dynamic loading due to the mainshock (MS);
- Dynamic loading due to the aftershock (AS).

The first step is to derive fragility parameters for these events, based on the outputs of the FLAC analyses.

When considering tephra loading only, the numerical analyses (i.e., at step S2-2) show that DS₁ is reached with a static loading of 140 kPa. Assuming a standard deviation of 0.2 in order to accounting for modelling uncertainties, the corresponding fragility model is detailed in Table 2. The other limit state, DS₂, cannot be reached with the amount of static loading applied here.

Table 2: Fragility parameters estimated for the tephra loading.

	α_{TL} [kPa]	β_{TL}
DS ₁	140	0.2
DS ₂	-	-

Regarding the fragility function for the mainshock, a parametric fragility model is built by considering single-IM fragility curves at various levels of tephra loading (between 0 and 140 kPa). The corresponding fragility parameters are detailed in Table 3.

Table 3: Fragility parameters estimated for the mainshock, given various levels of tephra loading.

Tephra loading	DS ₁		DS ₂	
	α_{MS} [m/s ²]	β_{MS}	α_{MS} [m/s ²]	β_{MS}
TL = 0 kPa	4.1813	0.2297	11.4189	0.1748
TL = 40 kPa	1.7007	0.3182	58.8795	0.3182
TL = 60 kPa	0.5202	0.4725	-	-
TL = 80 kPa	0.1617	0.5866	-	-
TL = 100 kPa	0.0137	0.6889	-	-
TL = 120 kPa	5.69 x 10 ⁻⁵	0.7921	-	-
TL = 140 kPa	1.85 x 10 ⁻⁶⁰	0.9350	-	-

From Table 3, it can be seen that increasing tephra loads accelerate the occurrence of DS₁; however due to stabilizing effects of such loads (due to the limits of the Mohr-Coulomb model used here), residual displacements induced by the mainshock become too small to reach DS₂, as soon as the tephra loading exceeds 40 kPa.

Finally, the fragility function for the aftershock is based on the concept of damage-state-dependent fragility (Réveillère et al., 2012): the analyses that have reached DS₁ during the

mainshock are selected in the regression in order to estimate the probability of reaching DS_2 during the aftershock, given a previous DS_1 state due to the mainshock. The corresponding fragility parameters are detailed in Table 4.

Table 4: Conditional fragility parameters estimated for the aftershock, given DS_1 during the mainshock, and given various levels of tephra loading. Larger tephra loads are not considered here because they do not result in the occurrence of DS_2 .

Tephra loading	$DS_{2,AS} DS_{1,MS}$	
	α_{AS} [m/s ²]	β_{AS}
TL = 0 kPa	7.0688	0.2090
TL = 40 kPa	58.8795	0.3182

Without any tephra loading, the mainshock-aftershock loading has significant effect on the vulnerability of the dyke; since it is seen that much lower PGA levels are needed to reach DS_2 in the aftershock phase, if the dyke has already been slightly damaged during the mainshock.

Once the single-IM fragility functions have been estimated as above, it is possible to assemble them in order to assess the fragility of the dyke system exposed to multiple types of loadings. To this end, a small Bayesian Network is assembled in order to organize the sequence of probabilistic events that govern the final damage state of the dyke. The Bayesian Network is composed of the following nodes (see Figure 26):

- TL: distribution of applied tephra loads;
- MS: distribution of PGA for the mainshock;
- AS: distribution of PGA for the aftershock;
- DS_i : intermediate damage state of the dyke, due to joint loadings of tephra and mainshock;
- DS_f : final damage state of the dyke, due to joint loadings of tephra and aftershock, and given the intermediate damage state.

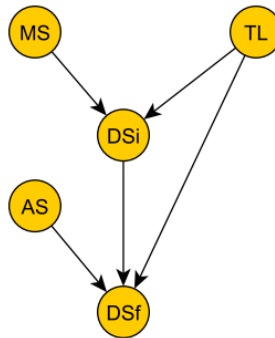


Figure 26: Bayesian Network for the construction of multi-hazard fragility models.

This approach follows the framework introduced by Gehl & D'Ayala (2016), where a Bayesian Network is developed to quantify the probability of various failure modes of a bridge exposed to multiple hazard loadings. The Bayesian Network is designed and solved with the BayesNet toolbox by Murphy (2001). The conditional probability tables of the nodes are constructed with the fragility parameters estimated above. Then, the nodes TL, MS and AS are evidenced at increasing sequential values: for each set of evidence, the Bayesian Network is solved and the corresponding probabilities $P(DS_f = DS_1 | TL, MS, AS)$ and $P(DS_f = DS_2 | TL, MS, AS)$ are extracted at the level of the DS_f node. It is finally possible to plot the evolution of these damage probabilities with respect to the various intensity measures. A few examples are shown below:

- Figure 27 to Figure 30: fragility surfaces with tephra load and mainshock PGA as intensity measures, for various levels of aftershock PGA;

- Figure 31 and Figure 32: fragility surfaces with mainshock and aftershock PGA as intensity measures, for various levels of tephra load.

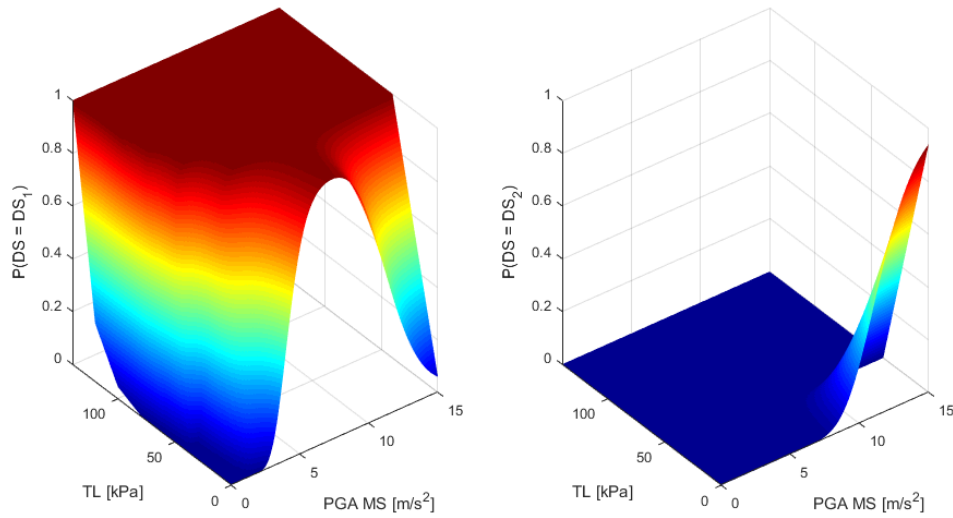


Figure 27: Probability of being in states DS_1 (Left) and DS_2 (Right) with respect to mainshock PGA (PGA MS) and tephra load (TL), with no aftershock.

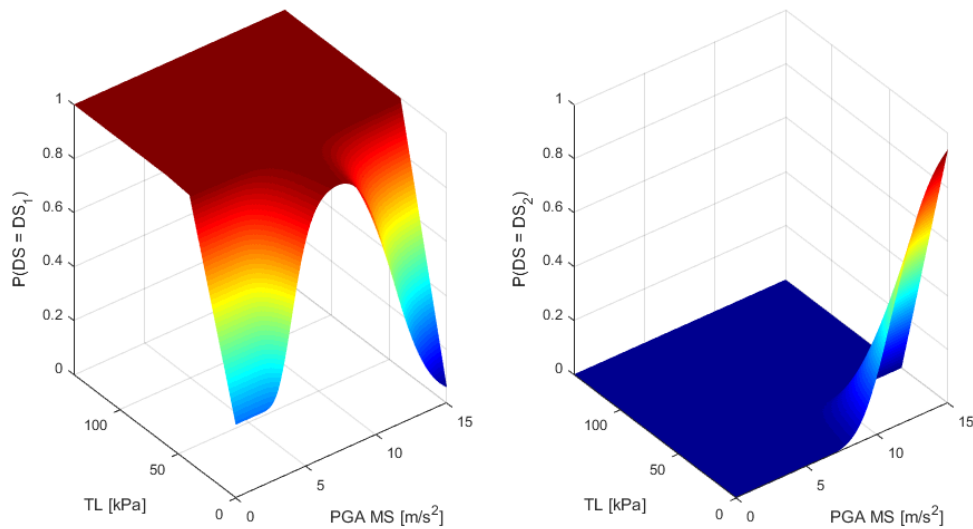


Figure 28: Probability of being in states DS_1 (Left) and DS_2 (Right) with respect to mainshock PGA (PGA MS) and tephra load (TL), with aftershock PGA = 3.64 m/s².

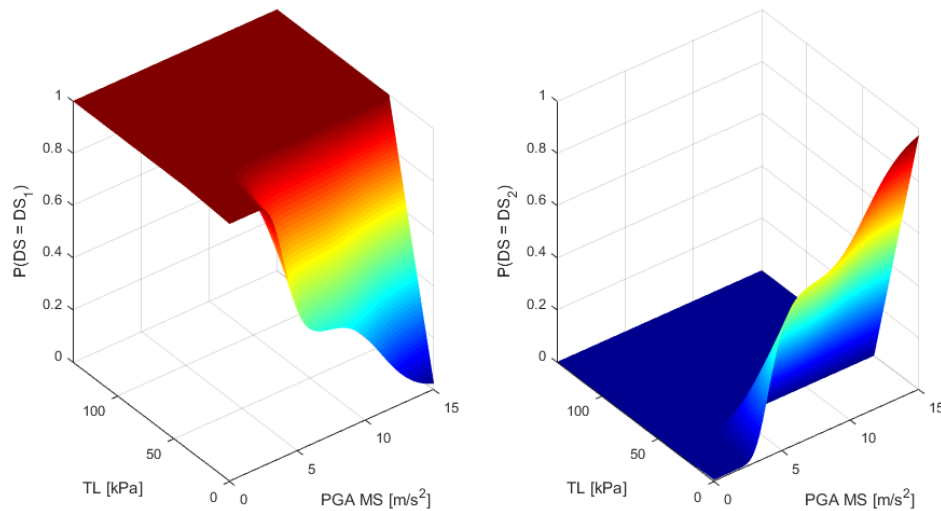


Figure 29: Probability of being in states DS_1 (Left) and DS_2 (Right) with respect to mainshock PGA (PGA MS) and tephra load (TL), with aftershock PGA = 7.42 m/s².

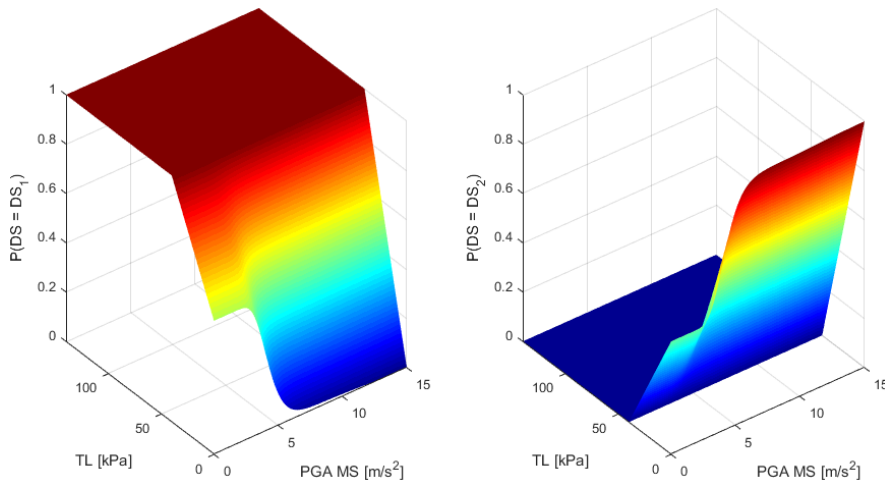


Figure 30: Probability of being in states DS_1 (Left) and DS_2 (Right) with respect to mainshock PGA (PGA MS) and tephra load (TL), with aftershock PGA = 11.21 m/s².

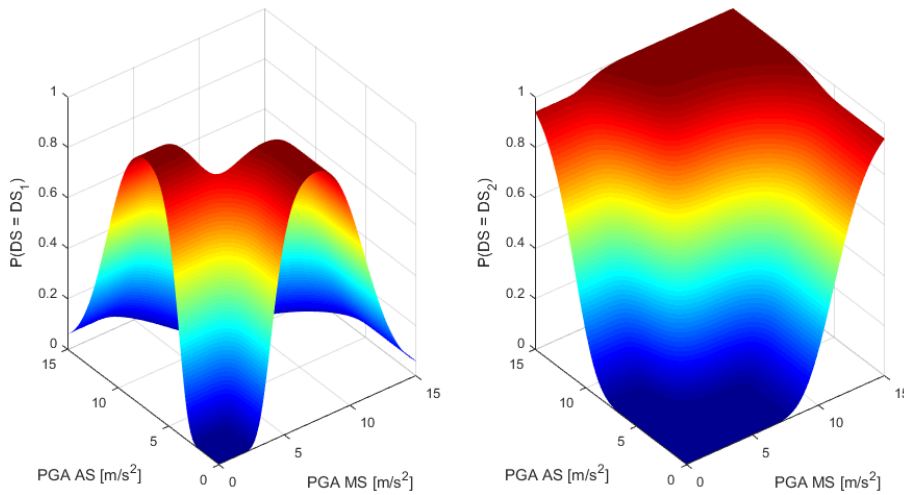


Figure 31: Probability of being in states DS_1 (Left) and DS_2 (Right) with respect to mainshock PGA (PGA MS) and aftershock PGA (PGA AS), with no tephra load.

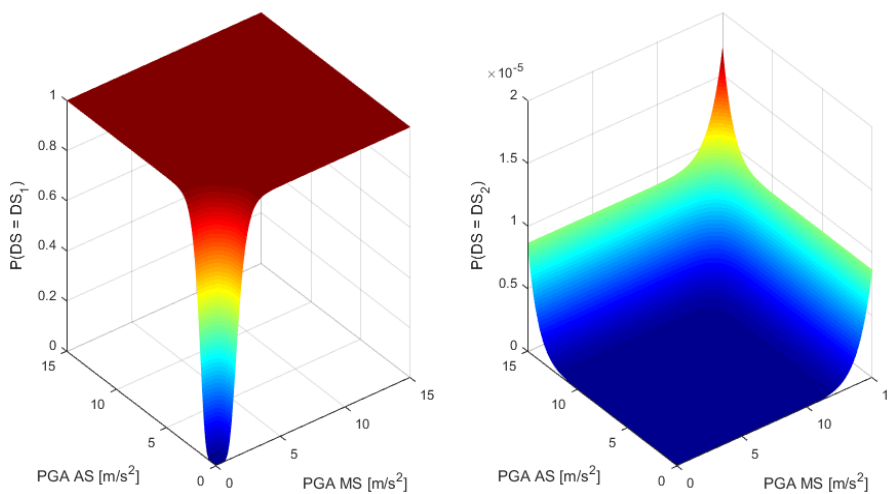


Figure 32: Probability of being in states DS_1 (Left) and DS_2 (Right) with respect to mainshock PGA (PGA MS) and aftershock PGA (PGA AS), with tephra load TL = 40 kPa.

From the figures above, we see that the proposed multi-hazard fragility functions, assembled from single-IM parametric fragility curves via a BN, have the potential to explore the effects of a wide range of hazard combinations. Coupled with probabilistic joint hazard models (WP1) and fault/event trees (WP3) in a PSA tool, they would shed a new light on potential issues due to the occurrence of coinciding or cascading external hazard events.

10 Conclusions

This report presents two multi-hazard analyses of a dyke. The first analysis considers three steps of loading involving (i) the site-specific coupled groundwater static-equilibrium conditions before earthquake, (ii) the earthquake scenario computed as a fully dynamic process, and (iii) a water level rise on the dyke's upstream reservoir potentially due to a failure of an upstream construction. The second analysis considers four steps of loading involving (i) the site-specific coupled groundwater static-equilibrium conditions before a volcanic eruption, (ii) a tephra fall on the dyke, (iii) a first earthquake (mainshock), and (iv) a second earthquake (aftershock).

Concerning the "earthquake-flooding" scenario and under the current modelling assumptions, the earthquake loading controls the dyke's maximum residual displacements that can reach 44 cm along the X-component and 20 cm along the Y-component. The flooding would deserve a better modelling approach considering for instance debris flows hitting the dyke or erosion of the dyke due to the increase of debit. The dyke's dynamic response to earthquake loading could also be improved by considering advanced constitutive laws for the sand and clay as well as potential liquefaction of the sandy shells.

Concerning the "volcanic eruption-mainshock-aftershock" scenario and under the current modelling assumptions, the aftershocks mostly increase the dyke's maximum residual displacements. The tephra loading generates a confining pressure that prevents the dyke from large residual displacements.

Further analyses (parametric and/or sensitivity) would be required to assess the influence of the mechanical properties, of the yielding criterion, of the saturation, and of the initial soil moisture condition of the dyke on its dynamic response. Such analyses are out of the scope of this report but would be relevant to better understand the subsidence, the rupture mechanisms and the fragility of the dyke with regards to the proposed scenarios.

11 References

- Alipour, A., Shafei, B. and Shinozuka, M. (2012). Reliability-Based Calibration of Load and Resistance Factors for Design of RC Bridges under Multiple Extreme Events: Scour and Earthquake. *Journal of Bridge Engineering*, 18(5), 362–371.
- Clayton, R., & Engquist, B. (1977). Absorbing boundary conditions for acoustic and elastic wave equations. *Bulletin of the seismological society of America*, 67(6), 1529-1540.
- Dawson, E. M., Roth, W. H., & Drescher, A. (1999). Slope stability analysis by strength reduction. *Geotechnique*, 49(6), 835-840.
- Foti, S. and Sabia, D. (2011). Influence of foundation scour on the dynamic response of an existing bridge. *Journal of Bridge Engineering*, 16(2), 295–304.
- Gehl, P., & D'Ayala, D. (2016). Development of Bayesian Networks for the multi-hazard fragility assessment of bridge systems. *Structural Safety*, 60, 37-46.
- Goldstein, P., Dodge, D., Firpo, M., Minner, L., Lee, W. H. K., Kanamori, H., ... & Kisslinger, C. (2003). SAC2000: Signal processing and analysis tools for seismologists and engineers. *The IASPEI international handbook of earthquake and engineering seismology*, 81, 1613-1620.
- Kawakami, F., & Asada, A. (1966). Damage to the ground and earth structures by the Niigata earthquake of June 16, 1964. *Soils and Foundations*, 6(1), 14-30.
- Itasca Consulting Group, Inc. (2019) *FLAC — Fast Lagrangian Analysis of Continua*, Ver. 8.1. Minneapolis: Itasca.
- Murphy, K. (2001). The Bayes net toolbox for Matlab. *Computing Science and Statistics*, 33, 1024-1034.
- Lee, K. and Rosowsky, D. (2006). Fragility analysis of woodframe buildings considering combined snow and earthquake loading. *Structural Safety*, 28(3), 289–303.
- Réveillère, A., Gehl, P., Seyed, D., & Modaressi, H. (2012). Development of seismic fragility curves for mainshock-damaged reinforced-concrete structures. In *15th World Conference on Earthquake Engineering*.
- Zuccaro, G., Cacace, F., Spence, R. J. S. and Baxter, P. J. (2008). Impact of explosive eruption scenarios at Vesuvius. *Journal of Volcanology and Geothermal Research*, 178(3), 416–423.

Appendix: FLAC/FISH configuration file of the “earthquake-flooding” scenario

The FLAC configuration file used for this study is distributed under the terms of the GNU GPL Licence. The terms are the following:

The program is a FLAC configuration file of the dyke problem design for the WP2.3 of H2020 NARSIS project Grant Agreement No. 755439.
Copyright (C) 2021 H2020 NARSIS - Contact: f.demartin at brgm.fr

This program is free: you can redistribute it and/or modify it under the terms of the GNU General Public License as published by the Free Software Foundation, either version 3 of the License, or (at your option) any later version.

This program is distributed in the hope that it will be useful, but WITHOUT ANY WARRANTY; without even the implied warranty of MERCHANTABILITY or FITNESS FOR A PARTICULAR PURPOSE. See the GNU General Public License for more details. You should have received a copy of the GNU General Public License along with this program. If not, see <http://www.gnu.org/licenses/>.

The FLAC configuration file is the following:

```
new
config gwflow dynamic
```

```
TITLE
H2020 NARSIS Project
```

```
set log on
set log results\flac.log
```

```
*****
;
;----Initialisation of the coordinate of the points (in m) defining the embankment----
*****
;
```

```
def para_geom
```

```
    array coord(7,3)
```

```
    coord(1,1) = -100.0 ;left boundary of domain
    coord(1,2) = -100.0 ;left boundary of domain
    coord(1,3) = -100.0 ;left boundary of domain
```

```
    coord(2,1) = -20.0 ;left boundary of embankment base (up stream)
    coord(2,2) = -20.0 ;left boundary of embankment base
    coord(2,3) = -5.0 ;left boundary of embankment crest
```

```
    coord(3,1) = -6.0 ;left boundary of core base
    coord(3,2) = -6.0 ;left boundary of core base
    coord(3,3) = -1.0 ;left boundary of core crest
```

```
    coord(4,1) = 0.0 ;middle of embankment
    coord(4,2) = 0.0 ;middle of embankment
    coord(4,3) = 0.0 ;middle of embankment
```

```

coord(5,1) = +6.0 ;right boundary of core base
coord(5,2) = +6.0 ;right boundary of core base
coord(5,3) = +1.0 ;right boundary of core crest

```

```

coord(6,1) = +20.0 ;right boundary of embankment base (down stream)
coord(6,2) = +20.0 ;right boundary of embankment base
coord(6,3) = +5.0 ;right boundary of embankment crest

```

```

coord(7,1) = +100.0 ;right boundary of domain
coord(7,2) = +100.0 ;right boundary of domain
coord(7,3) = +100.0 ;right boundary of domain

```

;array coord is duplicated into single variable because arrays do not seem to be accepted by
FLAC command like gen, etc.

```

x11 = coord(1,1)
x12 = coord(1,2)
x13 = coord(1,3)

```

```

x21 = coord(2,1)
x22 = coord(2,2)
x23 = coord(2,3)

```

```

x31 = coord(3,1)
x32 = coord(3,2)
x33 = coord(3,3)

```

```

x41 = coord(4,1)
x42 = coord(4,2)
x43 = coord(4,3)

```

```

x51 = coord(5,1)
x52 = coord(5,2)
x53 = coord(5,3)

```

```

x61 = coord(6,1)
x62 = coord(6,2)
x63 = coord(6,3)

```

```

x71 = coord(7,1)
x72 = coord(7,2)
x73 = coord(7,3)

```

```

y1 = -100.0
y2 = 0.0
y3 = 5.0

```

```

yMidPool = y2+(y3-y2)/2.0 ;water level before earthquake loading
yFullPool = y3 ;water level after earthquake loading

```

```

end
para_geom

```

```

*****
;-----Parameters to create the mesh and to define specific grid points (water level rise, etc.)
*****
;

```

```
def para_grid
```

```
    dx = 2.0
    dy = 2.0
```

```
;number of zones along x-direction (horizontal)
```

```
    array absDist(6,3)
```

```
    loop i (1,6)
        loop j (1,3)
            absDist(i,j) = int(abs(coord(i+1,j) - coord(i,j))/dx)
        end_loop
    end_loop
```

```
;number of zones along y-direction (vertical)
```

```
    nj12 = int((y2-y1)/dy)
    nj23 = int((y3-y2)/dy)
```

```
;j location of the level MidPool and FullPool
```

```
    njMidPool = int((yMidPool -y1)/dy) + 1
    njFullPool = int((yFullPool-y1)/dy) + 1
```

```
;start index of nodes wrt global numbering
```

```
    ni1 = 1
    ni2 = ni1 + absDist(1,1)
    ni3 = ni2 + absDist(2,1)
    ni4 = ni3 + absDist(3,1)
    ni5 = ni4 + absDist(4,1)
    ni6 = ni5 + absDist(5,1)
    ni7 = ni6 + absDist(6,1)
```

```
    ni2m1 = ni2 - 1
    ni3m1 = ni3 - 1
    ni4m1 = ni4 - 1
    ni5m1 = ni5 - 1
    ni6m1 = ni6 - 1
    ni7m1 = ni7 - 1
```

```
    ni6p1 = ni6 + 1
```

```
    nj1 = 1
    nj2 = nj1 + nj12
    nj3 = nj2 + nj23
```

```
    nj2m1 = nj2 - 1
    nj3m1 = nj3 - 1
```

```
;---grid size
```

```
    nc = ni7 - 1
    nl = nj3 - 1
```

```
end
para_grid
```

```
*****
;
;----Location of receivers----
*****
;
```

```
def receivers
```

```
;receiver#1 bedrock bottom free field
  xrec1 = int((x21 - x11)/2.0/dx)
  yrec1 = nj1
```

```
;receiver#2 bedrock free surface free field
  xrec2 = int((x21 - x11)/2.0/dx)
  yrec2 = nj2
```

```
;receiver#3 dyke basement clay
  xrec3 = int((x41 - x11)/dx)
  yrec3 = nj2 - 1
```

```
;receiver#4 dyke middle clay
  xrec4 = int((x41 - x11)/dx)
  yrec4 = nj3 - 1
```

```
;receiver#5 bedrock bottom below dyke
  xrec5 = int((x41 - x11)/dx)
  yrec5 = int((y3+y2)/2.0/dy)
```

```
;receiver#6 dyke middle sand_ustream
  emb_slope_ustream = (y3-y2)/(x23-x22)
  xrec6 = ni2 + int( ((x23-x22)/2.0)/dx )
  yrec6 = nj2 + int( ((x23-x22)/2.0*emb_slope_ustream)/dy )
```

```
;receiver#7 dyke middle sand_dstream
  xrec7 = ni5 + int( ((x62-x63)/2.0)/dx )
  yrec7 = yrec6
```

```
;receiver#8 bedrock middle free field
  xrec8 = int((x21 - x11)/2.0/dx)
  yrec8 = int(nj2/2)
```

```
;receiver#9 bedrock middle below dyke
  xrec9 = int((x41 - x11)/dx)
  yrec9 = int(nj2/2)
```

```
end
receivers
```

```
*****
;
;----init array to be used to save maximum along x, y direction
;and xy modulus (array used by routine final_disp.fis)----
*****
;
```

```
def init_array_ff
```

```

        array ff(3)

        ff(1) = string(0.0)
        ff(2) = string(0.0)
        ff(3) = string(0.0)

end
init_array_ff
;*****
;-----init routine to get maximum displacement
;*****
def init_gpf

    igpf = igp
    jgpf = jgp

end

def init_get_max

    max_disp_x = 0.0
    max_disp_y = 0.0
    max_disp_xy = 0.0

end

def get_final_disp

    loop i (1,igpf)
        loop j (1,jgpf)
            max_disp_x = max(max_disp_x,abs(xdisp(i,j)))
        endloop
    endloop

    loop i (1,igpf)
        loop j (1,jgpf)
            max_disp_y = max(max_disp_y,abs(ydisp(i,j)))
        endloop
    endloop

    loop i (1,igpf)
        loop j (1,jgpf)
            max_disp_xy = max(max_disp_xy,abs(disp(i,j)))
        endloop
    endloop

end

def write_final_disp

    ff(1) = string(max_disp_x)
    ff(2) = string(max_disp_y)
    ff(3) = string(max_disp_xy)

```



```

ios = open(fname,1,1)
ios = write(ff,3)
ios = close

end

*****
;
;-----Construction of the model-----
*****
;

grid nc nl

gen x11 y1 x13 y3 x73 y3 x71 y1

;temporary initialisation of the model. The model is then changed to Mohr-Coulomb.

model elas

;adjust zones for the bedrock

gen x11 y1 x12 y2 x22 y2 x21 y1 ratio 1.0,1.0 i=ni1,ni2 j=nj1,nj2
gen x21 y1 x22 y2 x32 y2 x31 y1 ratio 1.0,1.0 i=ni2,ni3 j=nj1,nj2
gen x31 y1 x32 y2 x42 y2 x41 y1 ratio 1.0,1.0 i=ni3,ni4 j=nj1,nj2
gen x41 y1 x42 y2 x52 y2 x51 y1 ratio 1.0,1.0 i=ni4,ni5 j=nj1,nj2
gen x51 y1 x52 y2 x62 y2 x61 y1 ratio 1.0,1.0 i=ni5,ni6 j=nj1,nj2
gen x61 y1 x62 y2 x72 y2 x71 y1 ratio 1.0,1.0 i=ni6,ni7 j=nj1,nj2

;adjust zones for the embankment

gen x12 y2 x13 y3 x23 y3 x22 y2 ratio 1.0,1.0 i=ni1,ni2 j=nj2,nj3
gen x22 y2 x23 y3 x33 y3 x32 y2 ratio 1.0,1.0 i=ni2,ni3 j=nj2,nj3
gen x32 y2 x33 y3 x43 y3 x42 y2 ratio 1.0,1.0 i=ni3,ni4 j=nj2,nj3

gen x42 y2 x43 y3 x53 y3 x52 y2 ratio 1.0,1.0 i=ni4,ni5 j=nj2,nj3
gen x52 y2 x53 y3 x63 y3 x62 y2 ratio 1.0,1.0 i=ni5,ni6 j=nj2,nj3
gen x62 y2 x63 y3 x73 y3 x72 y2 ratio 1.0,1.0 i=ni6,ni7 j=nj2,nj3

*****
;
;-----Nullify left and right zones-----
*****
;

model null i ni1 ni2m1 j nj2 nj3m1

model null i ni6 ni7m1 j nj2 nj3m1

*****
;
;-----Create group corresponding to material---
*****
;

group 'bedrock' i=ni1,ni7m1 j=nj1,nj2m1

group 'sand_ustream' i=ni2,ni3m1 j=nj2,nj3m1

group 'clay_core' i=ni3,ni5m1 j=nj2,nj3m1

```



```

;pre-compute the pore pressures and stresses automatically for a model containing a
phreatic surface
call lnav.fis
set wth=y2 k0x=0.5 k0z=0.5
ininv

```

```

;check the equilibrium state and save it
history 999 unbalanced
solve elastic

```

```

;plot sigma_yy
window -110 110 -110 110 square on
set output 'results\1_static_init_wo_embankment_syy.jpg'
set plot jpg color size 1920 1080 ;set once and for all
plot pen syy fill

```

```

window -30 30 -30 30 square on
set output 'results\1_static_init_wo_embankment_syy_zoom.jpg'
plot pen syy fill

```

```

*****
;
;Static initialisation with embankment
*****
;

```

```

;embankment construction in one stage
model mohr group 'sand_dstream' ;vs = 400 m/s vp=800 m/s
prop density=1800.0 bulk=768.0E6 shear=288.0E6 cohesion=4000.0 friction=35.0
dilation=0.0 tension=0.0 group 'sand_dstream'

```

```

model mohr group 'sand_ustream' ;vs = 400 m/s vp=800 m/s
prop density=1800.0 bulk=768.0E6 shear=288.0E6 cohesion=4000.0 friction=35.0
dilation=0.0 tension=0.0 group 'sand_ustream'

```

```

model mohr group 'clay_core'
prop density=1800.0 bulk=768.0E6 shear=288.0E6 cohesion=4000.0 friction=35.0
dilation=0.0 tension=0.0 group 'clay_core'

```

```

solve

```

```

;plot sigma_yy
window -110 110 -110 110 square on
set output 'results\2_static_init_wi_embankment_syy.jpg'
plot pen syy fill

```

```

window -30 30 -30 30 square on
set output 'results\2_static_init_wi_embankment_syy_zoom.jpg'
plot pen syy fill

```

```

*****
;
;Static initialisation with embankment and water level rise to midpool (solve ground water
flow)
*****
;

```

```

; Raising Reservoir Level to mid pool

```

```

def compute_pp_mid_pool
    ppMidPool = abs(wdens * (yMidPool - y1) * ygrav) ;taking the absolute value because
pore-pressure is positive (convention)
end
compute_pp_mid_pool
print ppMidPool

;apply pore-pressure and fix pore-pressure boundary conditions
apply pp 0.0 var 0.0 ppMidPool from ni2,njMidPool to 1,1
fix pp i ni2    j njMidPool,nj3
fix pp i ni2, ni6 j nj3
fix pp i ni6    j nj2,nj3
fix pp i ni6, ni7 j nj2

set mechanical=off
set flow=on
water bulk=2.15E+9
set fastwb=on
set step 100000000
solve

;plot pore-pressure
window -110 110 -110 110 square on
set output 'results\3_static_init_wi_embankment_mid_pool_pp.jpg'
plot pen pp fill

window -30 30 -30 30 square on
set output 'results\3_static_init_wi_embankment_mid_pool_pp_zoom.jpg'
plot pen pp fill

.*****
;
;Static initialisation with embankment and water level rise to midpool (solve mechanical
pressure)
.*****
;

;mechanical pressure to represent the weight of the reservoir water
def compute_water_weight_mid_pool
    waterWeightMidPoll = abs(wdens * (yMidPool - y2) * ygrav) ;taking the absolute value
because "apply pressure" is positive (convention)
end
compute_water_weight_mid_pool
print waterWeightMidPoll

apply pressure 0.0 var 0.0 waterWeightMidPoll from ni2,njMidPool to 1,nj2
set mechanical=on
set flow=off
water bulk=0.0
solve

;plot sigma_yy
window -110 110 -110 110 square on
set output 'results\3_static_init_wi_embankment_mid_pool_water_weight_syy.jpg'
plot pen syy fill

window -30 30 -30 30 square on
set output 'results\3_static_init_wi_embankment_mid_pool_water_weight_syy_zoom.jpg'

```

plot pen syy fill

```
;plot effective sigma_yy
```

```
window -110 110 -110 110 square on
```

```
set output 'results\3_static_init_wi_embankment_mid_pool_water_weight_esyy.jpg'
```

```
plot pen esyy fill
```

```
window -30 30 -30 30 square on
```

```
set output 'results\3_static_init_wi_embankment_mid_pool_water_weight_esyy_zoom.jpg'
```

```
plot pen esyy fill
```

```
;plot pore-pressure
```

```
window -110 110 -110 110 square on
```

```
set output 'results\3_static_init_wi_embankment_mid_pool_water_weight_pp.jpg'
```

```
plot pen pp fill
```

```
window -30 30 -30 30 square on
```

```
set output 'results\3_static_init_wi_embankment_mid_pool_water_weight_pp_zoom.jpg'
```

```
plot pen pp fill
```

```
;
```

```
;plot displacements
```

```
window -110 110 -110 110 square on
```

```
set output 'results\3_xdisp.jpg'
```

```
plot pen xdisp fill
```

```
window -30 30 -30 30 square on
```

```
set output 'results\3_xdisp_zoom.jpg'
```

```
plot pen xdisp fill
```

```
window -110 110 -110 110 square on
```

```
set output 'results\3_ydisp.jpg'
```

```
plot pen ydisp fill
```

```
window -30 30 -30 30 square on
```

```
set output 'results\3_ydisp_zoom.jpg'
```

```
plot pen ydisp fill
```

```
window -110 110 -110 110 square on
```

```
set output 'results\3_xydisp.jpg'
```

```
plot pen xydisp fill
```

```
window -30 30 -30 30 square on
```

```
set output 'results\3_xydisp_zoom.jpg'
```

```
plot pen xydisp fill
```

```
;
```

```
*****
```

```
;compute maximum displacement among all the grid points
```

```
*****
```

```
call final_disp.fis ;call once and for all to init the functions
```

```
init_gpf
```

```
init_get_max
```

```

get_final_disp

set fname='results\3_max_disp.asc'

write_final_disp

*****
;
;----Dynamic simulation---
*****
;

;set dynamic time to zero to avoid large time coming from previous static analyses
SET dytime 0.0

;erase previous histories and numbering
HISTORY reset

;function to test "unit" impulse. Not used when a full seismogram is loaded into the dashspots
using HIST 10.
def wave
    if dytime > 1.0 / freq
        wave = 0.0
    else
        wave = 0.5 * (1.0 - cos(2.0*pi*freq * dytime))
    endif
end
set freq=50.0

;load seismogram (i.e., particle velocity) to be input in dashspot elements (equivalent to
paraxial element, zero order)
HIST 10 read acceleros\xa1.txt.gnu.dif.vel.sac.his

water bulk=2.15E+9
SET dyn on

INI xdis 0.0 ydis 0.0
INI xvel 0.0 yvel 0.0

APPLY ffield

;sanity set to ensure that x-dof are free at the bottom of the domain
FREE x j=1

APPLY xquiet j=1
APPLY yquiet j=1

;get the shear stress needed to inject the wave through the dashspots.
def get_input_syz

    voidRatio = porosity(1,1)/(1.0 - porosity(1,1))
    gsSpecific = density(1,1)/wdens
    gSat = ( voidRatio + gsSpecific ) / (1+voidRatio) * wdens
    vs_bedrock = sqrt(shear_mod(1,1)/density(1,1))
    inputSyx = -2.0*gSat*vs_bedrock

end

```

get_input_syz

APPLY sxy inputSyx HIST 10 j=1

```
*****
;
;----receivers---
*****
;
;receiver#1
HIST 100 xd i=xrec1 j=yrec1
HIST 101 xv i=xrec1 j=yrec1
HIST 102 xa i=xrec1 j=yrec1

;receiver#2
HIST 200 xd i=xrec2 j=yrec2
HIST 201 xv i=xrec2 j=yrec2
HIST 202 xa i=xrec2 j=yrec2
HIST 210 yd i=xrec2 j=yrec2
HIST 211 yv i=xrec2 j=yrec2
HIST 212 ya i=xrec2 j=yrec2

;receiver#3
HIST 300 xd i=xrec3 j=yrec3
HIST 301 xv i=xrec3 j=yrec3
HIST 302 xa i=xrec3 j=yrec3
HIST 303 sxy i=xrec3 j=yrec3

;receiver#4
HIST 400 xd i=xrec4 j=yrec4
HIST 401 xv i=xrec4 j=yrec4
HIST 402 xa i=xrec4 j=yrec4
HIST 403 sxy i=xrec4 j=yrec4
HIST 410 yd i=xrec4 j=yrec4
HIST 411 yv i=xrec4 j=yrec4
HIST 412 ya i=xrec4 j=yrec4

;receiver#5
HIST 500 xd i=xrec5 j=yrec5
HIST 501 xv i=xrec5 j=yrec5
HIST 502 xa i=xrec5 j=yrec5
HIST 503 sxy i=xrec5 j=yrec5

;receiver#6
HIST 600 xd i=xrec6 j=yrec6
HIST 601 xv i=xrec6 j=yrec6
HIST 602 xa i=xrec6 j=yrec6
HIST 603 sxy i=xrec6 j=yrec6

;receiver#7
HIST 700 xd i=xrec7 j=yrec7
HIST 701 xv i=xrec7 j=yrec7
HIST 702 xa i=xrec7 j=yrec7
HIST 703 sxy i=xrec7 j=yrec7

;receiver#8
HIST 800 xd i=xrec8 j=yrec8
```

```
HIST 801 xv i=xrec8 j=yrec8
HIST 802 xa i=xrec8 j=yrec8
```

```
;receiver#9
```

```
HIST 900 xd i=xrec9 j=yrec9
HIST 901 xv i=xrec9 j=yrec9
HIST 902 xa i=xrec9 j=yrec9
```

```

;
;
*****
;

```

```
;compute strain at receiver#6
```

```
*****
;

```

```
call strain_hist.fis
set irec=xrec6
set jrec=yrec6
strain_hist
HIST 604 str_rec
```

```
HIST 1 dytime
HIST nstep 1
```

```
HIST 1000 unbalanced
```

```
SOLVE dytime 30.0
```

```

;
;
*****
;

```

```
;plots
```

```
*****
;

```

```

;
;
;plot displacements
```

```
window -110 110 -110 110 square on
set output 'results\4_earthquake_loading_xdisp.jpg'
plot pen xdisp fill
```

```
window -30 30 -30 30 square on
set output 'results\4_earthquake_loading_xdisp_zoom.jpg'
plot pen xdisp fill
```

```
window -110 110 -110 110 square on
set output 'results\4_earthquake_loading_ydisp.jpg'
plot pen ydisp fill
```

```
window -30 30 -30 30 square on
set output 'results\4_earthquake_loading_ydisp_zoom.jpg'
plot pen ydisp fill
```

```
window -110 110 -110 110 square on
set output 'results\4_earthquake_loading_xydisp.jpg'
plot pen xydisp fill
```

```
window -30 30 -30 30 square on
set output 'results\4_earthquake_loading_xydisp_zoom.jpg'
plot pen xydisp fill
```



```

*
*
*****
;get final displacements and max
*****
*

init_get_max

get_final_disp

set fname='results\4_max_disp.asc'

write_final_disp

*
*
*****
;water level rise after earthquake loading
*****
*

;unset dynamic mode
set dyn off

;reset groundwater flow time
set gwttime 0.0

;update boundary condition from dynamic to static

;remove all mechanical (free field and quiet here) conditions but keep ground water
conditions (pore-pressure)
apply remove mech from ni1,nj1 to ni1,nj2
apply remove mech from ni7,nj1 to ni7,nj2

;remove quiet
apply remove mech j = 1

;init velocities before computation
INI xvel 0.0 yvel 0.0

;fix x-displacement on vertical boundaries (sanity fix because already done)
fix x i=ni1
fix x i=ni7

;fix xy-displacement on horizontal boundary (sanity fix because already done)
fix x y=j=nj1

*****
*
;Static initialisation with embankment and water level rise to fullpool (solve ground water
flow)
*****
*

; Raising Reservoir Level to mid pool
def compute_pp_full_pool
    ppFullPool = abs(wdens * (yFullPool - y1) * ygrav) ;taking the absolute value because
pore-pressure is positive (convention)
end

```

```
compute_pp_full_pool
print ppFullPool
```

```
;apply pore-pressure from the crest (ni3,njFullPool) to the bottom left of the domain (1,1) and
fix pore-pressure boundary conditions
```

```
apply pp 0.0 var 0.0 ppFullPool from ni2,njFullPool to 1,1
fix pp i ni2, ni6 j nj3
fix pp i ni6    j nj2,nj3
fix pp i ni6, ni7 j nj2
```

```
set dyn off
set mechanical=off
set flow=on
water bulk=2.15E+9
set fastwb=on
set step 100000000
solve
;save results\5_water_level_rise_gwflow.sav
```

```
;plot pore-pressure
window -110 110 -110 110 square on
set output 'results\5_water_level_rise_gwflow_pp.jpg'
plot pen pp fill
```

```
window -30 30 -30 30 square on
set output 'results\5_water_level_rise_gwflow_pp_zoom.jpg'
plot pen pp fill
```

```
*****
;
;Static initialisation with embankment and water level rise to fullpool (solve mechanical
pressure)
*****
;
```

```
;mechanical pressure to represent the weight of the reservoir water
def compute_water_weight
    waterWeightFullPoll = abs(wdens * (yFullPool - y2) * ygrav) ;taking the absolute value
because "apply pressure" is positive (convention)
end
compute_water_weight
print waterWeightFullPoll
```

```
apply pressure 0.0 var 0.0 waterWeightFullPoll from ni3,njFullPool to 1,nj2
set mechanical=on
set flow=off
water bulk=0.0
set sratio 1e-3 ;or increase convergence ratio to avoid rotation of the domain, like 1e-2
solve
save results\5_water_level_rise_mechanical.sav
```

```
;plot sigma_yy
window -110 110 -110 110 square on
set output 'results\5_water_level_rise_mechanical_syy.jpg'
plot pen syy fill
```

```
window -30 30 -30 30 square on
set output 'results\5_water_level_rise_mechanical_syy_zoom.jpg'
```

plot pen syy fill

```
;plot effective sigma_yy
window -110 110 -110 110 square on
set output 'results\5_water_level_rise_mechanical_esyy.jpg'
plot pen esyy fill
```

```
window -30 30 -30 30 square on
set output 'results\5_water_level_rise_mechanical_esyy_zoom.jpg'
plot pen esyy fill
```

```
;plot pore-pressure
window -110 110 -110 110 square on
set output 'results\5_water_level_rise_mechanical_pp.jpg'
plot pen pp fill
```

```
window -30 30 -30 30 square on
set output 'results\5_water_level_rise_mechanical_pp_zoom.jpg'
plot pen pp fill
```

```
;plot displacements
window -110 110 -110 110 square on
set output 'results\5_water_level_rise_mechanical_xdisp.jpg'
plot pen xdisp fill
```

```
window -30 30 -30 30 square on
set output 'results\5_water_level_rise_mechanical_xdisp_zoom.jpg'
plot pen xdisp fill
```

```
window -110 110 -110 110 square on
set output 'results\5_water_level_rise_mechanical_ydisp.jpg'
plot pen ydisp fill
```

```
window -30 30 -30 30 square on
set output 'results\5_water_level_rise_mechanical_ydisp_zoom.jpg'
plot pen ydisp fill
```

```
window -110 110 -110 110 square on
set output 'results\5_water_level_rise_mechanical_xydisp.jpg'
plot pen xydisp fill
```

```
window -30 30 -30 30 square on
set output 'results\5_water_level_rise_mechanical_xydisp_zoom.jpg'
plot pen xydisp fill
```

```
;
;
;*****
;
;get final displacements and max
;*****
;
```

init_get_max

get_final_disp

set fname='results\5_max_disp.asc'

write_final_disp

;close log file
set log off